Technical Article

A Circuit Interpretation of the Volume Integral Equation Method: the Partial Element Equivalent Circuit Approach

***Abstract* — A comprehensive review of the well-established Partial Element Equivalent Circuit (PEEC) method is given and the state–of–the–art of the method, with focus on the inclusion of conductive, dielectric, and magnetic media in the formulation, is discussed. Both the standard (structured) and unstructured PEEC discretizations are presented and discussed. Furthermore, the Amperian and the Coulombian formulation for the inclusion of magnetic media are presented and compared. Different solution strategies for the solution of the PEEC system of equations are also discussed. Moreover, the breakdown in frequency issue and strategies for its suppression are presented. Finally, the case study of a Near Field Communication antenna is considered as an example of the applicability of the formulation to problems of industrial interest. Comparisons with commercial software, measurements, and state–of–the–art PEEC methods are given. Sample codes are available at https://github.com/UniPD-DII-ETCOMP/DenseMatrixMarket**

I. Introduction

A large body of literature shows that integral equation methods (IEMs) are particularly suited for the solution of low and high frequency electromagnetic (EM) problems involving large domains with the characteristics of vacuum. Indeed, one of the most attractive features of IEMs is that the background domain (e.g. the air), in which the EM devices are placed, has not to be discretized. Thus, with respect of the Finite Element Method (FEM), IEMs allow for an easier discretization process and a reduction of the number of Degrees of Freedoms (DoFs).

On the other hand, one of the main drawbacks of IEMs is the generation of a dense linear system, which leads to an eventually unfeasible storage requirement and long computation time for its solution. However, the recent development of efficient data compression techniques based, e.g., on *Hierarchical*-matrices [1] with adaptive cross approximation (ACA) [2] has rejuvenated the interest on IEMs [3]. Among all the IEMs, the Partial Element Equivalent Circuit (PEEC) method, introduced by A. Ruehli in 1972 [4], has been shown to be well suited for the analysis of several EM devices, such as interconnects [5], [6] and antennas [7], [8]. PEEC is the subject of a large body of literature, e.g. one entire book [9], a book chapter [10], PhD theses [11], [12], [13] and a large number of scientific papers. One of the peculiar features of PEEC is the natural interpretation of the EM problem as a complex and fully coupled circuit problem. Thus, the coupling between discretized devices and lumped circuit components is straightforward and the final coupled EM-circuit problem can be solved, in principle, by means of a standard circuit solver based on the Modified Nodal Analysis (MNA) [14] technique.

Over the years, several research groups, e.g. from the University of L'Aquila (Italy) and ETH Zürich (Switzerland), have developed a multitude of extensions of what has become known as the *Standard*-PEEC method [15], [16].

In the standard approach, regular hexahedral and quadrilateral elements are usually adopted [9]. The unknowns of the problem, i.e. the current density and the charge density distributions, are represented by rectangular basis functions and the Electric Field Integral Equation (EFIE), combined with Ohm's law and the continuity equation, is then discretized by means of the Galerkin approach. The standard PEEC method was later extended to the more general case of non-orthogonal grids [17] through ad-hoc adjustments.

More recently, the *Unstructured*-PEEC method was introduced. This approach was initially presented in [18] for surface conductive models, and then extended to three-dimensional models and dielectric/magnetic media [19], [20]. This approach provides a theoretically sound formalization of PEEC, allowing the study of both structured and unstructured meshes without any particular additional effort. With the Unstructured-PEEC method the conservation properties of the EM unknowns are naturally and strongly imposed.

While conductive and dielectric media have been considered in the framework of PEEC quite early [19], [21], the extension to magnetic media has been achieved more recently, initially for quasi-static problems and later for the full wave case [22], [16], [20], [23], [15]. The first approaches presented in literature, proposed to solve a *magnetic equation* for the magnetic flux density together with the EFIE equation. Amperian currents [16], [20], or the magnetization [23], [15], were adopted as equivalent sources for the magnetic media. However, when this approach is embraced, the traditional PEEC elementary circuit cell [18] can be adopted only for the discretization of the electric domains and not for the magnetic ones, so that the circuit interpretation of the EM problem is partially lost. Moreover, when the properties of the magnetic unknowns (e.g. the magnetization) are to be strongly enforced, a method like the one proposed in [20] should be applied, with the drawback of increasing the number of unknowns.

More recently, a different approach based on the Coulombian interpretation of magnetization phenomena has been proposed in [24] and [25], with the aim of overcoming the drawbacks of the Amperian PEEC methods, and providing a re-collocation of PEEC in the context of IEMs. Indeed, such approach, which arises from a standard theoretical framework common to high-frequency IEMs, allows maintaining a strong circuit interpretation also in the presence of magnetic media.

The aim of this *Technical Article* is to provide a comprehensive review of the well-established PEEC method. Thus, both the standard and the unstructured PEEC discretization are first presented and discussed for conductive media only. Then, extensions of the PEEC formulation to dielectric and magnetic media are discussed. In this regard, two alternatives are presented and compared: the first based on the Amperian [20] and the second on the Coulombian [24] interpretation of magnetization phenomena.

The paper aims at showing that PEEC can be interpreted as a particular form of classical Volume Integral Equation methods and, at the same time, if appropriately formulated, maintains a strong circuit interpretation of the EM problem. In this regard, different solution strategies for the solution of the coupled EM-circuit problem are proposed and critically discussed.

Finally, as an example of the applicability of PEEC to problems of industrial interest, a real Near Field Communication (NFC) antenna [26] is simulated by means of both the Amperian and the Coulombian approaches. With the aim of showing the efficiency of PEEC combined with compression techniques, the NFC antenna problem is also solved by means of the HLIBPro library [27] based on Hierarchical-matrices and ACA.

II. Original PEEC Method for Conductive Media

In this section, with the aim of providing an easy and straightforward introduction for readers who are new to IEMs, the original PEEC method for homogeneous conductive media only is presented.
Thus, starting from the Maxwell's equations, the PEEC formulation is shortly derived and numerically discretized with two different approaches: the *Standard* one [9], which is the first procedure historically proposed and originally formulated for structured meshes only, and the *Unstructured* one (or *Dual* one) [18], which allows the study of structured and unstructured meshes without any particular additional effort.

A. Formulation

The conductive domain Ω_c, with boundary $\partial\Omega_c = \Gamma_c$, consists of all the regions with electrical conductivity σ_c greater than zero. The active, i.e. conductive, domain, which may consist of disjoint regions (i.e. $\Omega_c = \Omega_{c_1} \cup \cdots \cup \Omega_{c_n}$ where n is the number of distinct regions), is embedded in the inactive domain Ω_0 with the characteristics of vacuum. Considering only conductive media, all subregions of Ω_c are characterized by relative permittivity and permeability equal to one. The whole computational domain is given by $\Omega = \Omega_c \cup \Omega_0 = \mathbb{R}^3$.
For linear conductive media, Ohm's law holds:

$$\mathbf{E} = \rho_c \mathbf{J_c} \quad in\ \Omega_c, \tag{1}$$

where $\mathbf{E}$ is the electric field, $\rho_c = \sigma_c^{-1}$ is the electric resistivity, σ_c is the electric conductivity, and $\mathbf{J_c}$ is the conduction current density.
Maxwell's equations in the frequency domain can be written as:

$$\begin{aligned} \nabla \cdot \mathbf{E} &= \frac{\varrho_c}{\varepsilon_0}, \qquad \nabla \times \mathbf{E} = -i\omega\mathbf{B}, \\ \nabla \cdot \mathbf{B} &= 0, \quad \nabla \times \mathbf{H} = \mathbf{J_c} + i\omega\varepsilon_0\mathbf{E}, \end{aligned} \tag{2}$$

where ϱ_c is the free electric charge density, ε_0 is the permittivity of vacuum, $\mathbf{B}$ is the magnetic flux density, $\mathbf{H}$ is the magnetic field, i is the imaginary unit, $\omega = 2\pi f$ is the angular frequency and f is the frequency.
Moreover, the conduction current density and the charge density distributions must satisfy continuity laws in Ω_c and its boundary Γ_c:

$$\nabla \cdot \mathbf{J_c} = -i\omega\varrho_c, \quad \mathbf{J_c} \cdot \mathbf{n} = -i\omega\varsigma_c, \tag{3}$$

where ς_c is the free electric surface charge density which exists on Γ_c, i.e. the surface over which the current density is discontinuous. It is worth noting that the second expression in (3) only holds for homogeneous media, which is indeed the assumption in the present context.
A vector potential $\mathbf{A}$ and a scalar electric potential φ_e can then be introduced [28]:

$$\mathbf{E} = -i\omega\mathbf{A} - \nabla\varphi_e, \qquad \mathbf{B} = \nabla \times \mathbf{A}. \tag{4}$$

It is worth noting that in some communities $\mathbf{A}$ is referred to as *magnetic vector potential*, however, in order to avoid misunderstandings with other parts of the paper, $\mathbf{A}$ is here referred to simply as *vector potential*.

Applying the Lorenz gauge $\nabla \cdot \mathbf{A} = -i\omega\varepsilon_0\mu_0\varphi_e$, where μ_0 is the permeability of vacuum, and substituting (4) into (2), the following partial differential equation is obtained:

$$\Box\mathbf{A} = \mu_0\mathbf{J_c}, \tag{5}$$

where $\Box = (i\omega)^2 c_0^{-2} - \nabla^2$ is the d'Alembert operator and c_0 is the speed of light in vacuum.
The solution of (5) is:

$$\mathbf{A}(\mathbf{r}) = \mu_0 \int_{\Omega_c} \mathbf{J_c}(\mathbf{r}')\, g(\mathbf{r},\mathbf{r}')\, \mathrm{d}\Omega', \tag{6}$$

where $\mathbf{r}$ is the field point, $\mathbf{r}'$ is the integration point in Ω_c, and $g(\mathbf{r},\mathbf{r}')$ is the scalar *dynamic* Green's function [28]:

$$g(\mathbf{r},\mathbf{r}') = \frac{e^{-i\omega|\mathbf{r}-\mathbf{r}'|/c_0}}{4\pi|\mathbf{r}-\mathbf{r}'|}. \tag{7}$$

The scalar dynamic Green's function in (7), also known as *retarded* Green's function, represents the general solution of the fundamental Helmholtz equation. However, when the conductive domain is electrically short, the time delay effects in the propagation of the EM fields can be neglected and (7) can be replaced by

$$g(\mathbf{r},\mathbf{r}') = \frac{1}{4\pi|\mathbf{r}-\mathbf{r}'|}, \tag{7bis}$$

which is the *static* (or *non-retarded*) Green's function.

The integral expression of φ_e can be directly obtained from (5) by using the Lorenz gauge condition:

$$\varphi_e(\mathbf{r}) = \int_{\Omega_c} \frac{\varrho_c(\mathbf{r}')g(\mathbf{r},\mathbf{r}')}{\varepsilon_0}\mathrm{d}\Omega' + \int_{\Gamma_c} \frac{\varsigma_c(\mathbf{r}')g(\mathbf{r},\mathbf{r}')}{\varepsilon_0}\mathrm{d}\Gamma'. \tag{8}$$

The volume and surface charge densities in (8) can also be substituted with $\mathbf{J_c}$ resorting to (3).

Finally, from (4), the electric field $\mathbf{E}$ only depends on the conduction current density vector $\mathbf{J_c}$ by means of an integral relationship known as the *Electric Field Integral Equation* (EFIE) [29]:

$$\mathbf{E} = -i\omega\mathbf{A}(\mathbf{J_c}) - \nabla\varphi_e(\mathbf{J_c}) + \mathbf{E_{ext}}, \tag{9}$$

where $\mathbf{E_{ext}}$ is a known imposed field.
(9) together with (1) fully represent the EM problem, where $\mathbf{J_c}$ is the problem unknown. The formulation presented above is common to most Volume Integral Equation (VIE) methods [30], and for this reason the original PEEC formulation, which relies on them, can be interpreted as a particular VIE.

B. Discretization: Standard (Structured) Approach

The standard discretization procedure presented here is the basic and original form, while interested readers may consult more exhaustive references [9], [17]. With the aim of providing a general discussion, the 3-D case (i.e. volume discretization) is considered. Indeed, the discretization of 2-D (i.e. thin devices) and 1-D (i.e. thin wire devices) models can be easily derived from the 3-D one.
In the original PEEC formulation introduced by Ruheli in 1972 [4], conductive domains (which are the only active media considered in the original PEEC formulation) are subdivided into rectangular volume and surface cells, thus restricting the analysis to Manhattan-type model geometries.

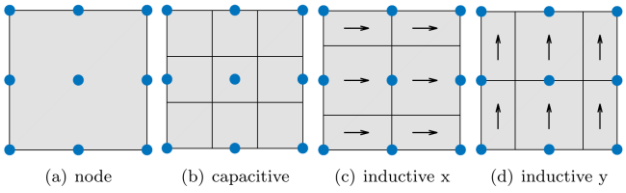

Fig. 1. Standard PEEC discretization in the 2-D case.

After obtaining a regular discretization of the conductive domains, a *capacitive* mesh and an interlocked *inductive* mesh, consisting of three distinct meshes oriented along the orthogonal axes, are defined.
Finally, the unknown current density vector and charge density distributions are approximated by pulse functions with support on the elements of the inductive and capacitive mesh, respectively.
For the sake of clarity, Fig. 1 shows a 2-D mesh discretization used to approximate the unknown current vector and charge distribution of a conductive structure of negligible thickness (e.g. a metallic chassis or a planar antenna).
The current density vector $\mathbf{J_c}$ is approximated by:

$$\mathbf{J_c}(\mathbf{r}) = \sum_k^{N_j} j_{c,k_s}\, \mathbf{p}_k(\mathbf{r}), \tag{10}$$

where N_j is the total number of inductive cells, $\mathbf{p}_k$ is the vector pulse basis function and j_{c,k_s} is the unknown DoF related to the *k*th element of the inductive mesh (the subscript *s* indicates the *Standard* PEEC discretization). The vector pulse functions $\mathbf{p}_k(\mathbf{r})$ are defined as:

$$\mathbf{p}_k(\mathbf{r}) = \begin{cases} A_k^{-1}\mathbf{u}_\gamma, & \mathbf{r} \in \Lambda_k \\ \mathbf{0}, & elsewhere \end{cases}, \tag{11}$$

where $\gamma = x, y, z$ depending on the *orientation* of the inductive mesh (see Fig. 1), $\mathbf{u}_\gamma$ is the unit vector along the direction γ, A_k is the cross section of the *k*th element of the inductive mesh, and Λ_k is the support of the *k*th basis function (i.e. the *k*th element of the inductive mesh).
The volume and surface charge densities, ϱ_c and ς_c, are approximated by:

$$\varrho_c(\mathbf{r}) = \sum_k^{N_q^v} q_{c,k_s}{}^v\, \mathrm{p}_k^{\mathrm{v}}(\mathbf{r}), \quad \varsigma_c(\mathbf{r}) = \sum_k^{N_q^s} q_{c,k_s}{}^s\, \mathrm{p}_k^{\mathrm{s}}(\mathbf{r}) \tag{12}$$

where $\mathrm{p}_k^{\mathrm{v}}$ and $\mathrm{p}_k^{\mathrm{s}}$ are the (scalar) pulse functions defined for the volume and surface capacitive cells, respectively, and $q_{s\,c,k}{}^v$ and $q_{s\,c,k}{}^s$ are the unknown DoFs related to the *k*th volume and surface element of the capacitive mesh, respectively. N_q^v and N_q^s are the number of volume and surface capacitive cells, respectively. Thus, ϱ_c and ς_c are discretized into N_q^v *volume* and N_q^s *surface capacitive cells*, respectively, by scalar pulse functions $\mathrm{p}_k^{\mathrm{v}}(\mathbf{r})$ and $\mathrm{p}_k^{\mathrm{s}}(\mathbf{r})$, defined as:

$$\mathrm{p}_k^{\mathrm{v}}(\mathbf{r}) = \begin{cases} V_k^{-1}, & \mathbf{r} \in \Lambda_{\mathrm{k}}^{\mathrm{v}} \\ 0, & elsewhere \end{cases}, \quad \mathrm{p}_k^{\mathrm{s}}(\mathbf{r}) = \begin{cases} A_k^{-1}, & \mathbf{r} \in \Lambda_{\mathrm{k}}^{\mathrm{s}} \\ \mathbf{0}, & elsewhere \end{cases} \tag{13}$$

where V_k is the volume of the *k*th volume-capacitive cell, A_k is the area of the *k*th surface-capacitive cell, $\Lambda_{\mathrm{k}}^{\mathrm{v}}$ is the support of $\mathrm{p}_k^{\mathrm{v}}$ (i.e. the volume-capacitive cell), and $\Lambda_{\mathrm{k}}^{\mathrm{s}}$ is the support of $\mathrm{p}_k^{\mathrm{s}}$ (i.e. the surface-capacitive cell).
Expansions (10) and (12) are then substituted into (8) and (9) and a Galerkin scheme is applied, that is (8) is tested with $\mathrm{p}_k^{\mathrm{v}}$ and $\mathrm{p}_k^{\mathrm{s}}$ and (9) is tested with $\mathbf{p}_k$, resulting in

$$\mathbf{e_{ext}}_s = \mathbf{R_s}\mathbf{j_{c_s}} + i\omega\mathbf{L_s}\mathbf{j_{c_s}} + \mathbf{G_{c_s}}\boldsymbol{\phi}_{e_s}, \tag{14}$$

$$\boldsymbol{\phi}_{e_s} = \mathbf{P_s}\mathbf{q_s}, \tag{15}$$

where:

- $\mathbf{e_{ext}}_s$ is a column vector with entries $e_{ext,h_s} = \int_\Omega \mathbf{p}_h(\mathbf{r}) \cdot \mathbf{E_{ext}}(\mathbf{r}) d\Omega$, for $h = 1, \cdots, N_j$,
- $\mathbf{R_s}$ is a $N_j \times N_j$ diagonal standard-PEEC *resistance matrix* with entries

$$R_{s_{h,k}} = \int_\Omega \rho_c(\mathbf{r})\mathbf{p}_h(\mathbf{r}) \cdot \mathbf{p}_k(\mathbf{r}) d\Omega, \tag{16}$$

- $\mathbf{j_{c_s}}$ is the column vector of the DoFs j_{c,k_s}, for $h = 1, \cdots, N_j$,
- $\mathbf{L_s}$ is an $N_j \times N_j$ dense standard-PEEC *inductance matrix* with entries

$$L_{s_{h,k}} = \mu_0 \int_\Omega \int_\Omega \mathbf{p}_h(\mathbf{r}) \cdot \mathbf{p}_k(\mathbf{r}') g(\mathbf{r}, \mathbf{r}') d\Omega' d\Omega, \tag{17}$$

- $\mathbf{G_{c_s}}$ is an $N_j \times (N_q^v + N_q^s)$ incidence matrix of the equivalent circuit obtained from the discretization of the conductive domain: each inductive cell is interpreted as a circuit branch connected to two circuit nodes (i.e. the nodes of the mesh).
- $\boldsymbol{\phi}_{e_s}$ is the column vector of the DoFs related to φ_e. $\boldsymbol{\phi}_{e_s}$ is subdivided into $\boldsymbol{\phi}_{e_s} = [\boldsymbol{\phi}_{e_s}^{\boldsymbol{v}}, \boldsymbol{\phi}_{e_s}^{\boldsymbol{s}}]$ where $\boldsymbol{\phi}_{e_s}^{\boldsymbol{v}} = \int_{\Omega_c} \mathrm{p}_k^v(\mathbf{r}) \varphi_e(\mathbf{r}) d\Omega$ for $k = 1, \cdots, N_q^v$, and $\boldsymbol{\phi}_{e_s}^{\boldsymbol{s}} = \int_{\Gamma_c} \mathrm{p}_k^s(\mathbf{r}) \varphi_e(\mathbf{r}) d\Omega$ for $k = 1, \cdots, N_q^s$; the scalar electric potential is instead related to the nodes of the mesh in a one-to-one relationship with the volume and surface cells of the capacitive mesh,
- $\mathbf{P_s}$ is a full $(N_q^v + N_q^s) \times (N_q^v + N_q^s)$ standard-PEEC *potential matrix* subdivided into

$$\mathbf{P_s} = \begin{bmatrix} \mathbf{P_s^{vv}} & \mathbf{P_s^{vs}} \\ \mathbf{P_s^{sv}} & \mathbf{P_s^{ss}} \end{bmatrix}, \tag{18}$$

where

$$P_{s,h,k}^{vv} = \varepsilon_0^{-1} \int_{\Omega_c} \int_{\Omega_c} \mathrm{p}_h^v(\mathbf{r})\, \mathrm{p}_k^v(\mathbf{r}') g(\mathbf{r}, \mathbf{r}') d\Omega' d\Omega, \tag{19}$$

$$P_{s,h,k}^{ss} = \varepsilon_0^{-1} \int_{\Gamma_c} \int_{\Gamma_c} \mathrm{p}_h^s(\mathbf{r})\, \mathrm{p}_k^s(\mathbf{r}') g(\mathbf{r}, \mathbf{r}') d\Gamma' d\Gamma, \tag{20}$$

$$P_{s,h,k}^{vs} = P_{s,k,h}^{sv} = \varepsilon_0^{-1} \int_{\Omega_c} \int_{\Gamma_c} \mathrm{p}_h^v(\mathbf{r})\, \mathrm{p}_k^s(\mathbf{r}') g(\mathbf{r}, \mathbf{r}') d\Gamma' d\Omega, \tag{21}$$

- $\mathbf{q_s}$ is the column vector of the DoFs related to ϱ_c and ς_c. $\mathbf{q_s}$ is subdivided into $\mathbf{q_s} = [\mathbf{q_s^v}, \mathbf{q_s^s}]$ where $\mathbf{q_s^v}$ are the DoFs $q_{s_k}^v$, for $k = 1, \cdots, N_q^v$, and $q_{s_k}^s$ is the DoFs q_k^s, for $k = 1, \cdots, N_q^s$.

In this discrete representation, $\mathbf{G_{c_s}}$ represents the algebraic equivalent of the gradient operator in (9). Moreover, since $\mathbf{j_{c_s}}$ are the fluxes of $\mathbf{J_c}$ through the cross sections of the inductive cells of the mesh and $\mathbf{q_s}$ are the electric charges enclosed in the capacitive cell of the mesh, the continuity equations (3) can be represented in an equivalent algebraic form as

$$\mathbf{G_{c_s}^T}\mathbf{j_{c_s}} = i\omega\mathbf{q_s}, \tag{22}$$

where $\mathbf{G_{c_s}^T}$ represents the algebraic equivalent of the divergence operator.
Since the vector pulse function $\mathbf{p}_k$ has a local support that coincides with the *k*th inductive mesh element, matrix $\mathbf{R_s}$ is a

diagonal matrix and the term $\mathbf{R_s j_{c_s}}$ in (14) can be interpreted as the ohmic voltage drop along the γ direction, with $\gamma = x, y, z$ depending on the orientation of the *k*th inductive mesh element. The matrix $\mathbf{L_s}$ is symmetric and is structured by three diagonal dense blocks:

$$\mathbf{L_s} = \begin{bmatrix} \mathbf{L_{xx}} & \mathbf{0} & \mathbf{0} \\ \mathbf{0} & \mathbf{L_{yy}} & \mathbf{0} \\ \mathbf{0} & \mathbf{0} & \mathbf{L_{zz}} \end{bmatrix} \tag{23}$$

Indeed, the inductance coefficient (17) vanishes when $\mathbf{p}_k$ and $\mathbf{p}_h$ have mutually orthogonal directions. The term $i\omega\mathbf{L_s j_{c_s}}$ in (14) can be interpreted as an inductive voltage drop due to the self and mutual inductive couplings between the elements of the inductive mesh.

Finally, the last term in (14) can be interpreted as a capacitive voltage drop obtained as the algebraic difference between the potentials of the terminal nodes of the inductive mesh elements (i.e. the circuit branches). In (15), the potentials are related to the electric charges by means of the dense symmetric potential matrix $\mathbf{P_s}$.

Following the circuit interpretation, (14) can be interpreted as the set of Kirchhoff's Voltage Law (KVL) written for each branch of the electric circuit.

The KVLs are complemented by the charge conservation law (22), i.e. by the Kirchhoff Current Laws (KCLs).

Moreover, (15) and (22) can be combined together resulting in

$$\mathbf{G_{c_s}^T j_{c_s}} - i\omega\mathbf{C}\boldsymbol{\phi}_{\mathbf{e_s}} = \mathbf{0}, \tag{24}$$

where $\mathbf{C} = \mathbf{P_s^{-1}}$ is defined as the *capacitance matrix*.

Finally, (14) and (24) can be assembled into a unique system of algebraic linear equations:

$$\begin{bmatrix} \mathbf{R_s} + i\omega\mathbf{L_s} & \mathbf{G_{c_s}} \\ \mathbf{G_{c_s}^T} & -i\omega\mathbf{C} \end{bmatrix} \begin{bmatrix} \mathbf{j_{c_s}} \\ \boldsymbol{\phi}_{e_s} \end{bmatrix} = \begin{bmatrix} \boldsymbol{e}_{ext_s} \\ \mathbf{0} \end{bmatrix}. \tag{25}$$

The linear system (25) features a complex symmetric matrix and generally enjoys good numerical properties (more details are given in section IV). However, $\mathbf{C}$ is obtained from the inverse of $\mathbf{P_s}$ and this operation requires a considerable computational cost which grows as $O\left(N_q^v + N_q^s\right)^3$.

However, by accepting the loss of symmetry, (25) can be also written in a form which avoids the inversion of $\mathbf{P_s}$:

$$\begin{bmatrix} \mathbf{R_s} + i\omega\mathbf{L_s} & \mathbf{G_{c_s}} \\ \mathbf{P_s}\,\mathbf{G_{c_s}^T} & -i\omega\mathbf{1} \end{bmatrix} \begin{bmatrix} \mathbf{j_{c_s}} \\ \boldsymbol{\phi}_{e_s} \end{bmatrix} = \begin{bmatrix} \boldsymbol{e}_{ext_s} \\ \mathbf{P_s} \cdot \mathbf{0} \end{bmatrix}. \tag{26}$$

where $\mathbf{1}$ denotes the identity matrix. Finally, (26) can also be reduced by eliminating $\boldsymbol{\phi}_{e_s}$ with the Schur complement approach [31]:

$$\left(\mathbf{R_s} + i\omega\mathbf{L_s} + \tfrac{1}{i\omega}\mathbf{G_{c_s}}\mathbf{P_s}\mathbf{G_{c_s}^T}\right)\mathbf{j_{c_s}} = \boldsymbol{e}_{ext_s}, \tag{27}$$

(27) is the discrete version of the continuum integral equation (9). This system is also complex symmetric and of a reduced size compared to (25) and (26). However, since ω appears at the denominator, it can be adopted only when the frequency is sufficiently larger than zero. Indeed, although the system is theoretically solvable for $\omega \neq 0$, the inductive term $i\omega\mathbf{L_s}$ and the capacitive term $\frac{1}{i\omega}\mathbf{G_{c_s}}\mathbf{P_s}\mathbf{G_{c_s}^T}$ scale differently with ω and for small values of the frequency. This different behavior often leads to the well-known *breakdown in frequency* problem [32], which is discussed in section IV.

The standard PEEC discretization scheme is based on an intuitive circuit interpretation of the continuum electromagnetic equations. However, the assumptions made in the derivation of the scheme sometimes lack of a systematic background and, in some circumstances, may lead to an inaccurate numerical method [18] since some properties of the EM unknowns are not strongly enforced. For these reasons, in the recent years the PEEC discretization scheme has been re-formulated introducing the concept of *duality* and *primal* and *dual* grids. In the next section, this more sound discretization approach, i.e. the unstructured PEEC discretization, is applied to the original PEEC formulation for the case of conductive homogeneous media only.

C. Discretization: Unstructured Approach

The unstructured PEEC discretization scheme has been introduced in [18] for surface conductive models. In that paper the concepts of primal and dual grids, typical of the Cell Method [33], [34], were applied in the framework of the PEEC method. Fig. 2 shows the unstructured PEEC discretization for the case of a conductive structure of negligible thickness. The unstructured PEEC discretization was then extended to the case of volume conductive and dielectric media [19]. For the sake of generality, the 3-D case is here considered. The 2-D and 1-D cases can be easily derived from the 3-D one.

In the unstructured discretization approach, the conductive domain Ω_c is discretized into a tetrahedral or hexahedral mesh, i.e. the *primal* grid. Then, a *dual* grid is obtained by taking the barycentric subdivision of the primal one, leading to a one-to-one relationship between the entities of the primal and the dual grid (e.g. primal volumes to dual nodes, primal faces to dual edges, etc.). Fig. 3 shows the primal and dual grids for a particular case of a hexahedral mesh. In this particular case, both the primal and the dual grids consist of hexahedral elements, whereas, for a general unstructured primal grid, the dual grid consists of generic polyhedra.

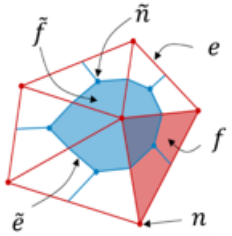

Fig. 2. Unstructured 2-D discretization. Primal gird: red. Dual grid: blue. *Primal* and *dual* geometric entities are indicated without and with *tilde*, respectively. Courtesy of Prof. Fabio Freschi, Politecnico di Torino, Italy.

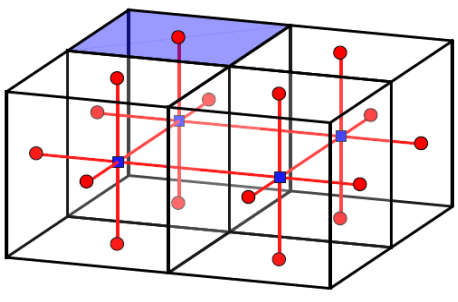

Fig. 3. Primal grid: black lines. Dual grid: red lines. Dual nodes: blue squared points in a one-to-one relationship with the primal volumes. Dual *boundary* nodes: red circled points in a one-to-one relationship with the primal *boundary* faces (one of them is highlighted in blue).

Then, the conduction current density vector is expanded by means of Whitney face elements, as:

$$\mathbf{J_c}(\mathbf{r}) = \sum_k^{N_f} j_{c,k}\, \mathbf{w}_k(\mathbf{r}), \tag{28}$$

where $\mathbf{w}_k$ is the *k*th Whitney face shape function related to the *k*th face of the mesh, i.e. $f_{c,k}$, $j_{c,k}$ is the flux of $\mathbf{J_c}$ through $f_{c,k}$ and N_{fc} is the number of faces of the mesh (i.e. primal faces). The $j_{c,k}$ are coefficients in an array $\mathbf{j_c}$. Whitney elements can be defined for both tetrahedra [35] or eight-node hexahedra (with planar quadrilateral faces) [36].
Whitney face elements enjoys the following properties

$$\nabla \cdot \mathbf{w}_k = \pm\tfrac{1}{V_h}, \qquad \mathbf{w}_k \cdot \mathbf{n} = \pm\tfrac{1}{A_k}, \tag{29}$$

where V_h is the volume of the element of the support of $\mathbf{w}_k$, $\mathbf{n}$ is the outward unit normal vector of $f_{c,k}$, and A_k is the area of $f_{c,k}$.
Thanks to properties (29), combining (3) with (28), expansions for the electric volume and surface free charges, which correspond to (12) for the standard PEEC, can be obtained. Thus, $\mathbf{q} = [\mathbf{q^v}, \mathbf{q^s}]$ related to the primal volumes and primal boundary faces of the mesh can be introduced also for the unstructured PEEC discretization.
Finally, (28) and (12) are substituted into (8) and (9) and a Galerkin scheme is applied, resulting in:

$$\mathbf{e}_{ext} = \mathbf{R}\mathbf{j_c} + i\omega\mathbf{L}\mathbf{j_c} + \mathbf{G_{\Omega c}}\boldsymbol{\phi}_e, \tag{30}$$

$$\boldsymbol{\phi}_e = \mathbf{P}\mathbf{q}. \tag{31}$$

It is worth noting that (30) and (31) are formally equivalent to (14) and (15), however, since $\mathbf{J_c}$ has been differently expanded (i.e. (28) instead of (10)) and the testing functions are now Whitney face elements instead of pulse functions (i.e. $\mathbf{w_k}$ instead of $\mathbf{p_k}$), the resistance, inductance and incidence matrices as well as the column vectors are defined differently, i.e.:

- $\mathbf{e}_{ext}$ is a column vector with entries $e_{ext,h} = \int_\Omega \mathbf{w}_h(\mathbf{r}) \cdot \mathbf{E_{ext}}(\mathbf{r}) d\Omega$, for $h = 1, \cdots, N_{fc}$,
- $\mathbf{R}$ is an $N_{fc} \times N_{fc}$ sparse unstructured-PEEC *resistance matrix* with entries

$$R_{h,k} = \int_{\mathbf{\Omega}} \mathbf{w}_h(\mathbf{r}) \cdot \mathbf{w}_k(\mathbf{r}) \rho_c(\mathbf{r}) d\Omega, \tag{32}$$

- $\mathbf{L}$ is an $N_{fc} \times N_{fc}$ full unstructured-PEEC *inductance matrix* with entries

$$L_{h,k} = \mu_0 \int_\Omega \int_\Omega \mathbf{w}_h(\mathbf{r}) \cdot \mathbf{w}_k(\mathbf{r}') g(\mathbf{r}, \mathbf{r}') d\Omega' d\Omega, \tag{33}$$

- $\mathbf{G_{\Omega c}}$ is an incidence matrix representing the algebraic equivalent of the gradient operator. $\mathbf{G_{\Omega c}}$ is $N_{fc} \times (N_{vc} + N_{fbc})$, where N_{vc} is the number of volume of the mesh and N_{fbc} is the number of boundary face of mesh. Each row of $\mathbf{G_{\Omega c}}$ related to an *internal* face, f_c^{int}, has +1 and −1 in the columns corresponding to the two tetrahedral (or hexahedral) elements sharing the face f_c^{int}. Instead, each row of $\mathbf{G_{\Omega c}}$ related to an *external* face, f_c^{ext}, has +1 in the column corresponding to the boundary face f_c^{ext}, and −1 in the column corresponding to the tetrahedral/hexahedral element having the face f_c^{ext}.
- $\boldsymbol{\phi}_e$ is a column vector with entries related to φ_e. $\boldsymbol{\phi}_e$ is subdivided into $\boldsymbol{\phi}_e = [\boldsymbol{\phi}_e^v, \boldsymbol{\phi}_e^s]$ where $\phi_{e_k}^v = \int_{\Omega_c} V_k^{-1}\, \varphi_e(\mathbf{r}) d\Omega$ for $k = 1, \cdots, N_{vc}$, and $\phi_{e_k}^s = \int_{\Gamma_c} A_k^{-1}(\mathbf{r}) \varphi_e(\mathbf{r}) d\Omega$ for $k = 1, \cdots, N_{fbc}$. V_k and A_k are the volume and the area of the *k*th primal volume and boundary face, respectively. The scalar electric potential is instead related to the dual nodes of the mesh in a one-to-one relationship with the primal volumes and primal boundary faces of the mesh,
- $\mathbf{P}$ is a full $(N_{vc} + N_{fbc}) \times (N_{vc} + N_{fbc})$ unstructured-PEEC *potential matrix* subdivided into

$$\mathbf{P} = \begin{bmatrix} \mathbf{P^{vv}} & \mathbf{P^{vs}} \\ \mathbf{P^{sv}} & \mathbf{P^{ss}} \end{bmatrix}, \tag{34}$$

in which

$$P_{h,k}^{vv} = \frac{1}{|\mathrm{v}_k||\mathrm{v}_h|\varepsilon_0} \int_{\mathrm{v}_k} \int_{\mathrm{v}_h} g(\mathbf{r}, \mathbf{r}') d\Omega' d\Omega, \tag{35}$$

$$P_{h,k}^{ss} = \frac{1}{|\mathrm{fb}_k||\mathrm{fb}_h|\varepsilon_0} \int_{\mathrm{fb}_k} \int_{\mathrm{fb}_h} g(\mathbf{r}, \mathbf{r}') d\Omega' d\Omega, \tag{36}$$

$$P_{h,k}^{vs} = \frac{1}{|\mathrm{v}_k||\mathrm{fb}_h|\varepsilon_0} \int_{\mathrm{v}_k} \int_{\mathrm{fb}_h} g(\mathbf{r}, \mathbf{r}') d\Omega' d\Omega, \tag{37}$$

$$P_{h,k}^{sv} = \frac{1}{|\mathrm{fb}_k||\mathrm{v}_h|\varepsilon_0} \int_{\mathrm{fb}_k} \int_{\mathrm{v}_h} g(\mathbf{r}, \mathbf{r}') d\Omega' d\Omega, \tag{38}$$

where v_k indicates the *k*th volume element of the mesh, fb_k the *k*th boundary face of the mesh, and $|\cdot|$ the measure.
- $\mathbf{q}$ is the column vector of the DoFs related to ϱ_c and ς_c. $\mathbf{q}$ is subdivided into $\mathbf{q} = [\mathbf{q^v}, \mathbf{q^s}]$ where $\mathbf{q^v}$ are the DoFs q_k^v, for $k = 1, \cdots, N_{vc}$, and $\mathbf{q^s}$ are the DoFs q_k^s, for $k = 1, \cdots, N_{fbc}$.

The evaluation of the inductance and potential coefficients requires the computation of double volume or surface integrals. When the support of the basis and the test functions overlap, the integrand exhibits a singularity due to the Green's function. Thus, singularity extraction techniques (as the ones proposed in [37] and [38]) should be adopted in order to accurately evaluate the matrix coefficients.
As in the standard discretization process presented in section II.B, $\mathbf{j_c}$ and $\mathbf{q}$ can be related by means of a discrete continuity equation obtained by inserting (28) in (3) and exploiting (29), i.e.

$$\mathbf{G_{\Omega c}^T}\mathbf{j_c} = i\omega\mathbf{q}. \tag{39}$$

Finally, even if the matrices and the column vectors are differently defined, the set of matrix equations (30), (31), and (39) is completely equivalent to (14), (15), and (22) of the standard PEEC discretization. Thus, the same considerations of section II.B still hold for the unstructured PEEC discretization and systems of equations equivalent to (25) and (27) can be easily derived.
The unstructured discretization offers a natural circuit interpretation of the EM problem. Indeed, the dual nodes (in a one-to-one relationship with the primal volumes and primal boundary faces of the mesh) can be interpreted as electric circuit nodes, whereas the dual edges (in a one-to-one relationship with the faces of the mesh) are interpreted as electric circuit branches. Thus, the structure of the PEEC elementary circuit cell, represented in Fig. 4, can be adopted to represent the equivalent circuit derived from the unstructured discretization process.

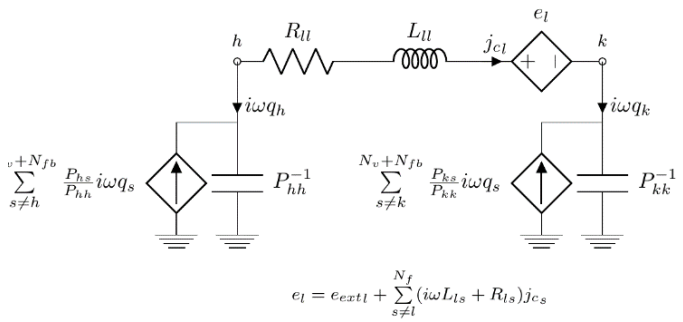

Fig. 4. Elementary PEEC circuit cell for the *l*th face of the mesh (i.e. the *l*th circuit branch).

D. Coupling PEEC and Lumped Circuits

One of the most attractive features of PEEC is the strong and natural circuit interpretation of the electromagnetic problem. Indeed, whether the standard or unstructured discretization schemes are adopted, the final matrix equations can be regarded as KVLs and KCLs written for each branch and node of the equivalent circuit, respectively.

Thus, electrical connections between the discretized devices and electric circuits consisting of lumped components such as voltage sources, resistors, inductors, capacitors can be easily considered.

In such a case, (25) is modified as follows by introducing the KVLs and KCLs written for each extra lumped circuit branch and node, i.e.

$$\begin{bmatrix} \mathbf{R}+i\omega\mathbf{L} & \mathbf{G_{\Omega c}} & \mathbf{0} & \mathbf{0} \\ \mathbf{G_{\Omega c}^T} & -i\omega\mathbf{P^{-1}} & \mathbf{G_{l,c}^T} & \mathbf{0} \\ \mathbf{0} & \mathbf{G_{l,c}} & \mathbf{Z}_l & \mathbf{G_{l,l}} \\ \mathbf{0} & \mathbf{0} & \mathbf{G_{l,l}^T} & \mathbf{0} \end{bmatrix} \begin{bmatrix} \mathbf{j_c} \\ \boldsymbol{\phi_e} \\ \mathbf{j_l} \\ \boldsymbol{\phi}_{\mathbf{e,l}} \end{bmatrix} = \begin{bmatrix} \boldsymbol{e_{ext}} \\ \boldsymbol{j_0} \\ \boldsymbol{e_{ext,l}} \\ \boldsymbol{j_{0,l}} \end{bmatrix}. \tag{40}$$

where $\mathbf{j_l}$ is a column vector storing the currents flowing in the lumped circuit branches, $\boldsymbol{\phi}_{\mathbf{e,l}}$ is a column vector storing the electric potentials of the lumped circuit nodes, $\mathbf{G_{c,l}}$ is an $N_l \times (N_{vc} + N_{f_{bc}})$ incidence matrix describing the connections between the N_l lumped circuit branches and the dual nodes of the discretized devices, and $\mathbf{G_{l,l}}$ is an $N_l \times N_n$ incidence matrix describing the connections between the N_l lumped circuit branches and the N_n lumped circuit nodes. $\boldsymbol{e_{ext,l}}$ is a column vector array storing the electric field applied to the lumped branches, $\boldsymbol{j_0}$ and $\boldsymbol{j_{0,l}}$ are column vectors storing external currents injected into the circuit nodes of the meh and lumped circuit nodes, respectively. $\mathbf{Z}_l$ is an $N_l \times N_l$ impedance matrix related to the lumped branches.

It is worth noting that the Schur complement approach can be applied also to (40) and thus $\boldsymbol{\phi}_\mathbf{e}$ can be explicitly removed from the unknowns.

III. Extensions of the PEEC Method: Dielectric, Magnetic, and Inhomogeneous Media

In this section, the PEEC method, presented above for homogeneous conductive media only, is extended to dielectric, magnetic, and inhomogeneous media following the most significant approaches proposed in literature [24], [25]. For the sake of conciseness, from now on only the unstructured PEEC discretization is considered, however, similar results can be obtained with the standard structured approach.

A. Dielectric Media

The extension of the PEEC method to dielectric media (i.e. media with relative electric permittivity ε_r other than the one of vacuum, $\varepsilon_r \neq 1$) can be achieved straightforwardly. Historically, the extension to dielectric media was first presented in [39].

The main idea, common to classical IEMs, is to replace the dielectric domain Ω_d (i.e. the regions with $\varepsilon_r \neq 1$) with an equivalent electric polarization density distribution in vacuum, i.e.

$$\mathbf{D} = \varepsilon_0\varepsilon_r\mathbf{E} = \varepsilon_0\mathbf{E} + \mathbf{P_e}, \tag{41}$$

where $\mathbf{D}$ is the electric displacement and $\mathbf{P_e}$ is the electric polarization vector.

With the help of (41), Maxwell's equations become:

$$\begin{aligned} \nabla\cdot\mathbf{E} &= \tfrac{\varrho_c+\varrho_p}{\varepsilon_0}, & \nabla\times\mathbf{E} &= -i\omega\mathbf{B}, \\ \nabla\cdot\mathbf{B} &= 0, & \nabla\times\mathbf{H} &= \mathbf{J_c} + \mathbf{J_p} + i\omega\varepsilon_0\mathbf{E}, \end{aligned} \tag{42}$$

where $\mathbf{J_p} = i\omega\mathbf{P_e}$ is the polarization current vector and ϱ_p is the volume bound electric charge density which is related to $\mathbf{J_p}$ by means of

$$\nabla\cdot\mathbf{J_p} = -i\omega\varrho_p, \quad \mathbf{J_p}\cdot\mathbf{n} = -i\omega\varsigma_p, \tag{43}$$

where ς_p is the electric bound surface charge density on $\Gamma_d = \partial\Omega_d$, i.e. the surface over which $\mathbf{J_p}$ is discontinuous.

A constitutive equation which relates $\mathbf{E}$ with $\mathbf{J_p}$ can be introduced and derived from (41), i.e.

$$\mathbf{E} = \rho_d\mathbf{J_p}, \quad in\ \Omega_d, \tag{44}$$

where

$$\rho_d = \tfrac{1}{i\omega\varepsilon_0(\varepsilon_r-1)}, \quad in\ \Omega_d, \tag{45}$$

is the equivalent electric resistivity of dielectric domains.

From (42)-(45), it is clear that, from a mathematical point of view, $\mathbf{J_p}$ acts in the same way as $\mathbf{J_c}$. Thus, the electrical current density vector $\mathbf{J_e} = \mathbf{J_c} + \mathbf{J_p}$ and the electric charge densities $\varrho_e = \varrho_c + \varrho_p$ and $\varsigma_e = \varsigma_c + \varsigma_p$ can be introduced in the electric domain $\Omega_\mathrm{e} = \Omega_c \cup \Omega_d$. Moreover, the electric resistivity ρ_e equal to

$$\rho_e = \tfrac{1}{\sigma_c+i\omega\varepsilon_0(\varepsilon_r-1)}, \quad in\ \Omega_e, \tag{46}$$

can be introduced. Using (46), the whole discussion still holds for dielectric media by simply substituting $\mathbf{J_c}$ with $\mathbf{J_e}$, Ω_c with Ω_e, ρ_c with ρ_e, ϱ_c with ϱ_e, and ς_c with ς_e.

B. Magnetic Media: Amperian Interpretation

The extension of the PEEC method to magnetic media (i.e. media with relative magnetic permeability μ_r other than the one of vacuum, $\mu_r \neq 1$) has been obtained more recently. In this section, the extension of PEEC to magnetic media is achieved by following the Amperian interpretation of the magnetization phenomena, as first proposed in [22] for the standard PEEC

discretization and then in [20] for the Unstructured PEEC discretization.

As for the extension to dielectric media, the main idea is still to replace the magnetic domain Ω_m (i.e. the regions with $\mu_r \neq 1$) with an equivalent magnetization distribution in vacuum, i.e.

$$\mathbf{B} = \mu_0\mu_r\mathbf{H} = \mu_0\mathbf{H} + \mu_0\mathbf{M}, \tag{47}$$

where $\mathbf{M}$ is the magnetization vector.

From (4) and (47), $\mathbf{H} = \mu_0^{-1}\nabla \times \mathbf{A} - \mathbf{M}$ and thus (5) becomes

$$\Box\mathbf{A} = \boldsymbol{\mu_0}(\mathbf{J_c} + \boldsymbol{\nabla} \times \mathbf{M}) \tag{48}$$

whose solution (in the sense of distribution theory) is given by

$$\mathbf{A}(\mathbf{r}) = \mu_0 \int_{\Omega_c} \mathbf{J_c}\,(\mathbf{r}')g(\mathbf{r},\mathbf{r}')\mathrm{d}\Omega' + \mu_0 \int_{\Omega_m} \mathbf{J_a}\,(\mathbf{r}')g(\mathbf{r},\mathbf{r}')\mathrm{d}\Omega' + \mu_0 \int_{\Gamma_m} \mathbf{K_a}\,(\mathbf{r}')g(\mathbf{r},\mathbf{r}')\mathrm{d}\Gamma', \tag{49}$$

where $\mathbf{J_a} = \nabla \times \mathbf{M}$ and $\mathbf{K_a} = \mathbf{M} \times \mathbf{n}$ are the volume and surface *Amperian* currents, respectively, and $\Gamma_m = \partial\Omega_m$. The integral expression of φ_e can be obtained again by combining (49) with the Lorenz gauge condition. This leads again to (8). Indeed $\mathbf{J_a}$ and $\mathbf{K_a}$ (which are *electric* currents) are obtained from the curl of $\mathbf{M}$ and thus are divergence free. As a matter of fact, in ideal (non-conductive) magnetic media no free or bound electric charge is present, thus the presence of magnetic media does not directly affect the electric scalar potential.

Following the same idea of section II.A, where a constitutive relation between $\mathbf{E}$ and $\mathbf{J_c}$ has been imposed, a constitutive relation must now be imposed between $\mathbf{M}$ and $\mathbf{B}$, i.e.

$$\mathbf{B} = \alpha_m\mathbf{M}, \quad in\ \Omega_m. \tag{50}$$

where

$$\alpha_m = \frac{\mu_0\mu_r}{\mu_r - 1}, \quad in\ \Omega_m. \tag{51}$$

Finally, if conductive, dielectric, and magnetic media are considered, the whole EM problem can be reduced to

$$\rho_e\mathbf{J_e} = -i\omega\mathbf{A}(\mathbf{J_c},\mathbf{J_a},\mathbf{K_a}) - \nabla\varphi_e(\mathbf{J_e}) + \mathbf{E_{ext}}, \quad in\ \Omega_e, \tag{52}$$

$$\alpha_m\mathbf{M} = \nabla \times \mathbf{A}(\mathbf{J_c},\mathbf{J_a},\mathbf{K_a}) + \mathbf{B_{ext}}, \quad in\ \Omega_m. \tag{53}$$

where $\mathbf{B_{ext}}$ is the imposed magnetic flux density field.

(52) and (53) can then be discretized following the standard or the unstructured procedure proposed in [22] or [20], respectively.

By choosing the unstructured scheme of [20], after discretizing Ω_m with tetrahedra (or hexahedra), $\mathbf{M}$ is expanded by means of Whitney edge shape functions, i.e.

$$\mathbf{M}(\mathbf{r}) = \sum_k^{N_{em}} m_k\,\mathbf{w_k^e}(\mathbf{r}), \tag{54}$$

where $\mathbf{w_k^e}$ is the *k*th Whitney edge shape function [35] related to the *k*th edge of the mesh, i.e. $e_{m,k}$, m_k is the line integral of $\mathbf{M}$ along $e_{m,k}$ and N_{em} is the number of edges of the mesh (i.e. primal edges). Thus, the column vector $\mathbf{m}$, with entries m_k with $k = 1,\cdots,N_{em}$, is defined.

By substituting the expansions (28) and (54) in (52) and (53), and applying a Galerkin approach (i.e. (52) is tested with $\mathbf{w_k}$ where $k = 1,\cdots,N_{fc}$, and (53) is tested with $\mathbf{w_k^e}$ where $k = 1,\cdots,N_{em}$) the following system of equations is obtained (more details can be found in [20] and [24]):

$$\begin{bmatrix} \mathbf{R} + i\omega\mathbf{L} & \mathbf{G_{\Omega c}} & \mathbf{i\omega}[\mathbf{L_{e,ja}}\mathbf{L_{e,ka}}]\begin{bmatrix}\mathbf{C_{\Omega m}}\\ \mathbf{C_{\Gamma m}}\end{bmatrix} \\ \mathbf{G_{\Omega sc}^T} & -i\omega\mathbf{P^{-1}} & \mathbf{0} \\ \begin{bmatrix}\mathbf{C_{\Omega m}}\\ \mathbf{C_{\Gamma m}}\end{bmatrix}^T[\mathbf{L_{ej_a}}\mathbf{L_{ek_a}}]^T & \mathbf{0} & \mathbf{F} - \begin{bmatrix}\mathbf{C_{\Omega m}}\\ \mathbf{C_{\Gamma m}}\end{bmatrix}^T\begin{bmatrix}\mathbf{L_{ja,ja}} & \mathbf{L_{ja,ka}}\\ \mathbf{L_{ka,ja}} & \mathbf{L_{ka,ka}}\end{bmatrix}\begin{bmatrix}\mathbf{C_{\Omega m}}\\ \mathbf{C_{\Gamma m}}\end{bmatrix} \end{bmatrix}\begin{bmatrix}\mathbf{j_c}\\ \boldsymbol{\phi_e}\\ \mathbf{m}\end{bmatrix} = \begin{bmatrix}\boldsymbol{e_{ext}}\\ \mathbf{0}\\ \boldsymbol{b_{ext}}\end{bmatrix}. \tag{55}$$

where the *volume*, *volume-surface*, and *surface* Amperian inductance matrices $\mathbf{L_{ej_a}}$, $\mathbf{L_{ek_a}}$, $\mathbf{L_{j_aj_a}}$, $\mathbf{L_{j_ak_a}}$, $\mathbf{L_{k_aj_a}}$, $\mathbf{L_{k_ak_a}}$ (which represent the discrete operators related to the volume and surface Amperian currents) are given by

$$L_{e,ja_{h,k}} = \mu_0 \int_{\Omega_e}\int_{\Omega_m} \mathbf{w}_h(\mathbf{r}) \cdot \mathbf{w}_k(\mathbf{r}')g(\mathbf{r},\mathbf{r}')d\Omega' d\Omega, \tag{56}$$

$$L_{e,ka_{h,k}} = \mu_0 \int_{\Omega_e}\int_{\Gamma_m} \mathbf{w}_h(\mathbf{r}) \cdot (\mathbf{n} \times \mathbf{w}_k^{\mathbf{e}}(\mathbf{r}'))g(\mathbf{r},\mathbf{r}')d\Gamma' d\Omega, \tag{57}$$

$$L_{ja,ja_{h,k}} = \mu_0 \int_{\Omega_m}\int_{\Omega_m} \mathbf{w}_h(\mathbf{r}) \cdot \mathbf{w}_k(\mathbf{r}')g(\mathbf{r},\mathbf{r}')d\Omega' d\Omega, \tag{58}$$

$$L_{ja,ka_{h,k}} = L_{ka,ja_{k,h}} = \mu_0 \int_{m}\int_{\Gamma_m} \mathbf{w}_h(\mathbf{r}) \cdot (\mathbf{n} \times \mathbf{w}_k^{\mathbf{e}}(\mathbf{r}'))g(\mathbf{r},\mathbf{r}')d\Gamma' d\Omega, \tag{59}$$

$$L_{ka\,,ka_{h,k}} = \mu_0 \int_{\Gamma_m}\int_{\Gamma_m} (\mathbf{n} \times \mathbf{w}_h^{\mathbf{e}}(\mathbf{r})) \cdot (\mathbf{n} \times \mathbf{w}_k^{\mathbf{e}}(\mathbf{r}'))g(\mathbf{r},\mathbf{r}')d\Gamma' d\Gamma. \tag{60}$$

In (55), $\mathbf{C_{\Omega m}}$ is the curl (faces to edges) incidence matrix of Ω_m of size $N_{fm} \times N_{em}$ (N_{fm} is the number of faces of the mesh of Ω_m), $\mathbf{C_{\Gamma m}}$ is the curl selection matrix of size $N_{e_bm} \times N_{em}$ which selects the boundary edges of Ω_m (N_{e_bm} is the number of boundary edges of Ω_m).

$\mathbf{F}$ of size $N_{em} \times N_{em}$ represents the discrete form of (50) given by

$$F_{h,k} = \int_{\mathbf{\Omega_m}} \alpha_m(\mathbf{r})\,\mathbf{w}_h^{\mathbf{e}}(\mathbf{r}) \cdot \mathbf{w}_k^{\mathbf{e}}(\mathbf{r})d\Omega, \tag{61}$$

while $\mathbf{b}_{ext}$ is the column vector with entries $b_{ext,h} = \int_\Omega \mathbf{w}_h^{\mathbf{e}}\,(\mathbf{r}) \cdot \mathbf{B_{ext}}(\mathbf{r})d\Omega$, for $h = 1,\cdots,N_{em}$.

The above discussion, based on the Amperian interpretation of magnetization phenomena, refers to the first approach proposed in literature for the extension of PEEC to magnetic media. It is worth noting that, when this approach is chosen, the discretization of the magnetic domain does not offer the same circuit interpretation by means of the traditional PEEC elementary circuit cell. Thus, the circuit interpretation of the whole electromagnetic problem becomes less evident [24].

Another important aspect which is worth noting is that this method suffers from a numerical issue when media with relatively high values of magnetic permeability are involved. Indeed, the constitutive relation (50) depends on α_m, which, with the increase of the relative permeability, tends to μ_0 (i.e. $\alpha_m \to \mu_0$ with increasing μ_r). For instance, from a numerical point of view, the difference between media with μ_r = 1,000 and μ_r= 10,000, due to round–off errors [40], may become indistinguishable when floating–point arithmetic is used. When $\mathbf{F}$ is summed to other integral matrices (which are affected by numerical approximations due to the integration of Green's function) this numerical issue is amplified. Indeed, the numerical approximations which affect the integral matrices are orders of magnitude greater than the last significant digits of α_m.

However, aside from these drawbacks, the Amperian method allows for an easy implementation. Indeed, as discussed in section IV.C, under some conditions, the volume Amperian

currents can be forced to be zero, thus improving the computational performances of the method.

C. Magnetic Media: Coulombian Interpretation

To solve the problems of the Amperian approach described above, a different approach based on the Coulombian interpretation of the magnetization phenomena has been proposed in [19], [41] and extensively in [24] where the Amperian and the Coulombian methods have also been compared. This approach is based on a theoretical framework which is quite common in the high frequency community, but less used for low frequency EM problems.
Maxwell's equations (considering conductive, dielectric, and magnetic media) are first rewritten in a symmetrized form [30]:

$$\begin{aligned} \nabla \cdot \mathbf{E} &= \frac{\varrho_e}{\varepsilon_0}, \quad -\nabla \times \mathbf{E} = \mathbf{J_m} + i\omega\mu_0\mathbf{H}, \\ \nabla \cdot \mathbf{H} &= \frac{\varrho_m}{\mu_0}, \quad \nabla \times \mathbf{H} = \mathbf{J_e} + i\omega\varepsilon_0\mathbf{E}, \end{aligned} \tag{62}$$

where $\mathbf{J_m} = i\omega\mu_0\mathbf{M}$ is the magnetic current density vector and ϱ_m is the volume bound magnetic charge density [42] which is related to $\mathbf{J_m}$ by means of

$$\nabla \cdot \mathbf{J_m} = -i\omega\varrho_m, \quad \mathbf{J_m} \cdot \mathbf{n} = -i\omega\varsigma_m, \tag{63}$$

where ς_m is the magnetic bound surface charge density on $\Gamma_m = \partial\Omega_m$, i.e. the surface over which $\mathbf{J_m}$ is discontinuous.
Then, a constitutive equation relating $\mathbf{H}$ to $\mathbf{J_m}$ can be introduced and derived from (47), i.e.

$$\mathbf{H} = \rho_m \mathbf{J_m}, \quad in\ \Omega_m, \tag{64}$$

where

$$\rho_m = \frac{1}{i\omega\mu_0(\mu_r - 1)}, \quad in\ \Omega_m, \tag{65}$$

is the equivalent magnetic resistivity of magnetic domains.
As is customary for high frequency IEMs, the *electric* and *magnetic* vector potentials $\mathbf{A}_e$ and $\mathbf{A}_m$, respectively, and the scalar electric and magnetic potentials φ_e and φ_m, respectively, are introduced [43]:

$$\mathbf{E} = -i\omega\mathbf{A}_e - \nabla\varphi_e - \varepsilon_0^{-1}\nabla \times \mathbf{A}_m, \tag{66}$$
$$\mathbf{H} = -i\omega\mathbf{A}_m - \nabla\varphi_m + \mu_0^{-1}\nabla \times \mathbf{A}_e. \tag{67}$$

$\mathbf{A}$, $\mathbf{A}_e$, and $\mathbf{A}_m$ are related by $\mathbf{A} = \mathbf{A}_e + (i\omega\varepsilon_0^{-1})\nabla \times \mathbf{A}_m$ and the Lorenz gauges $\nabla \cdot \mathbf{A_e} = -i\omega\varepsilon_0\mu_0\varphi_e$ and $\nabla \cdot \mathbf{A_m} = -i\omega\varepsilon_0\mu_0\varphi_m$ are imposed. Substituting (66) and (67) into (62), following partial differential equations are obtained:

$$\Box\mathbf{A_e} = \mu_0\mathbf{J_e} \tag{68}$$
$$\Box\mathbf{A_m} = \varepsilon_0\mathbf{J_m} \tag{69}$$

which are solved by:

$$\mathbf{A_e}(\mathbf{r}) = \mu_0 \int_{\Omega_e} \mathbf{J_e}(\mathbf{r}')g(\mathbf{r},\mathbf{r}')\mathrm{d}\Omega', \tag{70}$$
$$\mathbf{A_m}(\mathbf{r}) = \varepsilon_0 \int_{\Omega_m} \mathbf{J_m}(\mathbf{r}')g(\mathbf{r},\mathbf{r}')\mathrm{d}\Omega'. \tag{71}$$

By means of the Lorenz gauges, φ_e and φ_m can be obtained from (70) and (71). Thus, φ_e is still given by (8) by substituting ϱ_c with ϱ_e, $\varsigma_c$with ς_e, Ω_c with Ω_e, and Γ_c with Γ_e. φ_m is instead given by

$$\varphi_m(\mathbf{r}) = \int_{\Omega_m} \frac{\varrho_m(\mathbf{r}')g(\mathbf{r},\mathbf{r}')}{\mu_0}\mathrm{d}\Omega' + \int_{\Gamma_c} \frac{\varsigma_m(\mathbf{r}')g(\mathbf{r},\mathbf{r}')}{\mu_0}\mathrm{d}\Gamma'. \tag{72}$$

Thanks to the Coulombian interpretation and the introduction of the four potentials, the formulation benefits from a remarkable symmetry for electric and magnetic media. $\mathbf{J_m}$ can now be expanded as in (28) by means of Whitney face shape functions, leading to the corresponding column vector of DoFs $\mathbf{j_m}$. Then, the expansions of $\mathbf{J_e}$ and $\mathbf{J_m}$ are substituted in (66) and (67) and the resulting equations are tested with the same Whitney face shape functions. This finally results in:

$$\begin{bmatrix} \mathbf{R} + i\omega\mathbf{L} & \mathbf{G_{\Omega c}} & \mathbf{K_{em}} & \mathbf{0} \\ \mathbf{G_{\Omega c}^T} & -i\omega\mathbf{P_e^{-1}} & \mathbf{0} & \mathbf{0} \\ -\mathbf{K_{me}} & \mathbf{0} & \mathbf{R_m} + i\omega\mathbf{L_m} & \mathbf{G_{\Omega m}} \\ \mathbf{0} & \mathbf{0} & \mathbf{G_{\Omega m}^T} & -i\omega\mathbf{P_m^{-1}} \end{bmatrix} \begin{bmatrix} \mathbf{j_c} \\ \boldsymbol{\phi}_\mathbf{e} \\ \mathbf{j_m} \\ \boldsymbol{\phi}_\mathbf{m} \end{bmatrix} = \begin{bmatrix} \mathbf{e_{ext}} \\ \mathbf{0} \\ \mathbf{h_{ext}} \\ \mathbf{0} \end{bmatrix}, \tag{73}$$

where $\boldsymbol{\phi}_\mathbf{m}$ is the array of DoFs corresponding to φ_m, $\mathbf{h_{ext}}$ is the array of DoFs related to $\mathbf{H_{ext}}$, matrices $\mathbf{R_m}$, $\mathbf{L_m}$, $\mathbf{P_m}$ are the corresponding magnetic PEEC resistance, inductance, and potential PEEC matrices, respectively, given by

$$R_{m_{h,k}} = \int_{\Omega_m} \mathbf{w}_h(\mathbf{r}) \cdot \mathbf{w}_k(\mathbf{r})\rho_m(\mathbf{r})d\Omega, \tag{74}$$
$$L_{m_{h,k}} = \varepsilon_0 \int_{\Omega_m}\int_{\Omega_m} \mathbf{w}_h(\mathbf{r}) \cdot \mathbf{w}_k(\mathbf{r}')g(\mathbf{r},\mathbf{r}')d\Omega' d\Omega, \tag{75}$$
$$\mathbf{P_m} = \begin{bmatrix} \mathbf{P_m^{vv}} & \mathbf{P_m^{vs}} \\ \mathbf{P_m^{sv}} & \mathbf{P_m^{ss}} \end{bmatrix}, \tag{76}$$

where

$$P_{m,h,k}^{vv} = \frac{1}{|\mathrm{v}_k||\mathrm{v}_h|\mu_0}\int_{\mathrm{v}_k}\int_{\mathrm{v}_h} g(\mathbf{r},\mathbf{r}')d\Omega' d\Omega, \tag{77}$$

$$P_{m,h,k}^{ss} = \frac{1}{|\mathrm{fb}_k||\mathrm{fb}_h|\mu_0}\int_{\mathrm{fb}_k}\int_{\mathrm{fb}_h} g(\mathbf{r},\mathbf{r}')d\Omega' d\Omega, \tag{78}$$

$$P_{m,h,k}^{vs} = \frac{1}{|\mathrm{v}_k||\mathrm{fb}_h|\mu_0}\int_{\mathrm{v}_k}\int_{\mathrm{fb}_h} g(\mathbf{r},\mathbf{r}')d\Omega' d\Omega, \tag{79}$$

$$P_{m,h,k}^{sv} = \frac{1}{|\mathrm{fb}_k||\mathrm{v}_h|\mu_0}\int_{\mathrm{fb}_k}\int_{\mathrm{v}_h} g(\mathbf{r},\mathbf{r}')d\Omega' d\Omega. \tag{80}$$

$\mathbf{K_{em}} = \mathbf{K_{me}^T}$ are instead interaction matrices between electric and magnetic domains, with coefficients given by

$$K_{em_{h,k}} = \int_{\Omega_e}\int_{\Omega_m} \mathbf{w}_h(\mathbf{r}) \cdot \left(\frac{\boldsymbol{w}_k(\mathbf{r}')\times(\mathbf{r}-\mathbf{r}')}{|\mathbf{r}-\mathbf{r}'|^3} + i\omega\frac{\boldsymbol{w}_k(\mathbf{r}')\times(\mathbf{r}-\mathbf{r}')}{c_0|\mathbf{r}-\mathbf{r}'|^2}\right)d\Omega' d\Omega. \tag{81}$$

$\mathbf{G_{\Omega e}}$ and $\mathbf{G_{\Omega m}}$ are incidence matrices of Ω_e and Ω_m, respectively, defined analogously as $\mathbf{G_{\Omega c}}$.
The above formulation (which is more extensively presented in [24]) allows for a strong circuit interpretation also when magnetic media are considered. Indeed, the same PEEC elementary circuit cell of Fig. 4 can be adopted for electric and magnetic media by simply introducing the effects of matrices $\mathbf{K_{em}}$ and $\mathbf{K_{me}}$. Moreover, this method does not suffer from the numerical issue described for the Amperian approach when magnetic media with high value of magnetic permeability are considered.
The Schur complement can be again adopted for explicitly eliminating $\boldsymbol{\phi}_\mathbf{e}$ and $\boldsymbol{\phi}_\mathbf{m}$ from the unknowns of (73). Finally, when the frequency of the problem is relatively low, the inductive magnetic effects are almost negligible and the term $i\omega\mathbf{L_m}$ can be dropped.

D. Inhomogeneous Media

Up to now, homogeneous media only have been considered. As discussed in [24], when homogeneous media are considered, ϱ_p and ϱ_m vanish inside Ω_d and Ω_m. Instead, the presence of ϱ_c inside conductive media is a sensitive issue widely discussed in [44]. However, from an engineering point of view, ϱ_c is almost negligible for the whole frequency range.

The above PEEC formulations (Amperian and Coulombian) are obtained from the full Maxwell's equations and thus these conditions (i.e. the vanishing of ϱ_c, ϱ_p, and ϱ_m) are implicitly satisfied by (55) and (73), but not in a numerically strong sense. As mentioned in [21], when a VIE is solved for homogeneous media, the solution will be close to the exact one but the volume charge densities ϱ_p and ϱ_m will not be exactly zero inside Ω_d and Ω_m, particularly for mesh elements close to the boundaries Γ_d and Γ_m. Anyhow, this generally does not particularly affect the global quality of the solution, but in principle could be an issue when high accuracy is required. In section IV, a solution to strongly impose these conditions is given.

When inhomogeneous media are considered instead, the discretization process should be slightly modified as proposed in [24]. Two different kind of inhomogeneous media can be defined: 1) ε_r and μ_r are piecewise continuous functions, and 2) ε_r and μ_r are continuous smoothly varying functions in Ω_e and Ω_m. When the inhomogeneous medium is of kind 1), $\mathbf{J_e}$ and $\mathbf{J_m}$ have a discontinuity on the surface Γ^* which divides the two regions with different value of ε_r and μ_r. Thus, surface charges ς_e and ς_m appear on Γ^*. However, the Whitney face elements adopted for the expansion of $\mathbf{J_e}$ and $\mathbf{J_m}$ impose the continuity of the normal component. Instead, when the medium is of kind 2) the above PEEC formulations can still be used unmodified, taking care of evaluating the entries of the constitutive matrices with the value of ρ_e and ρ_m varying point-by-point. Alternatively, case 2) can be considered as a particular case of 1) by following [24].

For the sake of conciseness, the whole discussion is only summarized here and more details can be found in [24].

Following the circuit interpretation, inhomogeneous media are treated by replacing each circuit branch representing an interface face with two distinct branches connected to two floating nodes as exemplified in Fig. 5. The two floating nodes can be merged into a single interface node or remain distinct and considered as regular boundary faces. For both cases, each one of the two distinct branches can be represented by means of the traditional PEEC elementary circuit cell: one circuit node is the interior node placed in the barycenter of one of the two tetrahedral/hexahedral elements sharing the interface face, while the second circuit node coincides with one of the two floating nodes that can be merged into a single interface node or remain distinct.

Finally, it is worth noting that the above discussion does not consider the case of magnetic media for the Amperian PEEC method. However, the inhomogeneous magnetic media can be considered with the Amperian PEEC method by performing adjustments of the discretization scheme similar to the above ones [13].

E. Total Divergence-Free Currents Approach

A different approach for treating inhomogeneous media is the one first proposed in [19] for conductive and dielectric media and then extended to magnetic media in [25].

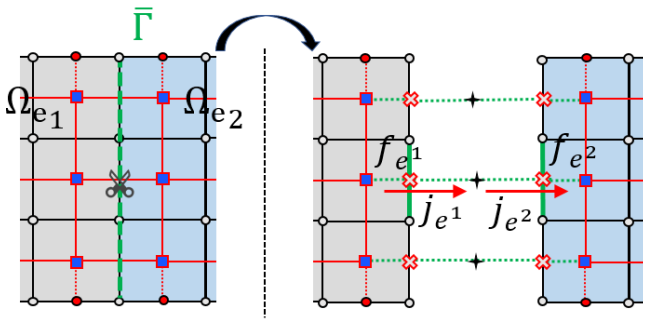

Fig. 5. Handling of inhomogeneous media: discretization adjustments.

Such approach introduces the total divergence-free electric and magnetic currents, i.e.

$$\mathbf{J_e^{tot}} = \mathbf{J_e} + i\omega\varepsilon_0\mathbf{E}, \qquad \mathbf{J_m^{tot}} = \mathbf{J_m} + i\omega\mu_0\mathbf{H}, \tag{82}$$

as unknowns of the EM problem. These currents are divergence-free for both homogeneous and inhomogeneous media. Thus, no particular care must be taken when inhomogeneous media are considered and no extra unknowns must be considered.

The drawback of this formulation is that, when $\mathbf{J_e^{tot}}$ and $\mathbf{J_e^{tot}}$ are considered as unknowns, the inductance and potential PEEC matrices depend on frequency dependent material coefficients. This formulation offers a circuit interpretation similar to the one of the Coulombian PEEC method.

However, when frequency sweep problems are considered, all matrices must be updated for each value of the frequency. Moreover, the coefficients of the potential matrices depend on the gradient of the Green's function, which exhibits a strong singularity which must be properly handled.

In the PEEC methods that use the currents and the magnetization as unknowns (i.e. $\mathbf{J_e}$, $\mathbf{J_m}$, and **M)** the inductance and potential matrices have useful numerical properties, i.e. they are related to the concepts of magnetic and electric energy. In this particular PEEC method, instead, because of the dependence of the integral matrices on the material parameters, these properties are less evident, since the inductance and potential matrices depend on the material properties of the media involved. However, this formulation is very general and allows for efficiently simulating complex EM devices in which inductive and capacitive effects are both significant, such as L-C-T components, as shown in [25].

IV. Solution of the PEEC System of Equations: Numerical Strategies and Issues

In this section, some numerical considerations concerning the PEEC systems of equations and different solution strategies are presented. For the sake of simplicity, most of the discussion is carried out considering conductive media only. However, equivalent considerations also apply in the case of dielectric and magnetic media.

A. PEEC System of Equations

In section II, the PEEC system of equations for conductive media only is presented in three different forms: 1) in (25) both currents and potentials are considered as unknowns, 2) in (26) both currents and potentials are considered as unknowns and the inversion of the potential matrix is avoided (losing the symmetry of the system), 3) in (27) only the currents are considered as unknowns leading to a more compact system.

Systems (25) and (26) (and also the more general (55), with the third row scaled by $i\omega$, and (73)) show good conditioning and do not suffer of breakdown in frequency. However, the large dimension of these systems leads to an interest in writing them in a more compact form, i.e. by using a reduced number of unknowns.
For this reason, when memory requirement is actually an issue, the more compact system (27) (obtained by means of the Schur complement approach) becomes more attractive. However, (27) suffers of a severe numerical issue which is due to the different scaling of the inductive and the capacitive term with ω, leading to the well-known *breakdown in frequency* issue.
However, as discussed in the next section, the breakdown in frequency issue can be avoided by using the well-known *loop-star* decomposition technique.

B. Change of Basis Technique

The final PEEC system of equations derived from the discretization of the Amperian and Coulombian formulations correctly enforces the EM properties of the unknowns, but not in a numerically strong sense. Indeed, the final discretized equations are obtained from the full Maxwell's equations; therefore, all the EM effects are considered. However, due to the discretization scheme, some of the properties of the unknowns (e.g. the divergence of the currents) are imposed by the integral matrices, which are affected by unavoidable numerical approximations.
As discussed in section III.D, the numerically weak imposition of the EM properties usually does not affect the global quality of the solution, but can in principle be an issue when high accuracy is required or when the actual distribution of the EM fields is important. Moreover, when some specific property need to be enforced (e.g. solenoidality), it is possible to adopt a change of basis in order to strongly impose such property and also reduce the number of the unknowns, i.e. the dimension of the final system to be solved. Furthermore, the loop-star change of basis technique can be adopted to avoid the problem of low frequency breakdown. In the following, this topic is only briefly discussed and interested readers can refer to more specific and exhaustive works in literature, e.g. in [32], [45].
The electric current density column vector $\mathbf{j_e}$ (or equivalently $\mathbf{j_m}$) can be decomposed as

$$\mathbf{j_e} = \mathbf{M}^{\circ}\mathbf{j}_\mathbf{e}^{\circ} + \mathbf{M}^{\star}\mathbf{j}_\mathbf{e}^{\star}, \tag{83}$$

where $\mathbf{M}^{\circ}$ is the *loop* matrix, $\mathbf{j}_\mathbf{e}^{\circ}$ is the column vector of independent *loop* currents, $\mathbf{M}^{\star}$ is the *star* matrix, and $\mathbf{j}_\mathbf{e}^{\star}$ is the column vector of independent *star* currents. The loop and star currents are defined as particular linear combinations of $\mathbf{j_e}$(i.e. the columns of $\mathbf{M}^{\circ}$ and $\mathbf{M}^{\star}$) as discussed in [32] and [45]. Matrices $\mathbf{M}^{\circ}$and $\mathbf{M}^{\star}$ must satisfy $\mathbf{M}^{\star\mathbf{T}}\mathbf{M}^{\circ} = \mathbf{0}$. $\mathbf{M}^{\circ}$and $\mathbf{M}^{\star}$ can be easily evaluated starting from the curl and divergence incidence matrices, respectively. However, when non simply connected domains or domains with cavities are considered, some particular care must be taken [19], [46]. By substituting (83) in (27) and projecting the resulting equations by means of the change of basis matrix $\mathbf{Q} = [\mathbf{M}^{\circ}, \mathbf{M}^{\star}]$, the following system is obtained:

$$\begin{bmatrix} \mathbf{M}^{\circ\mathbf{T}}[\mathbf{R} + i\omega\mathbf{L}]\mathbf{M}^{\circ} & \mathbf{M}^{\circ\mathbf{T}}[\mathbf{R} + i\omega\mathbf{L}]\mathbf{M}^{\star} \\ \mathbf{M}^{\star\mathbf{T}}[\mathbf{R} + i\omega\mathbf{L}]\mathbf{M}^{\circ} & \mathbf{M}^{\star\mathbf{T}}[\mathbf{R} + i\omega\mathbf{L} + \frac{\mathbf{1}}{i\omega}\mathbf{G}_{\mathbf{\Omega c}}\mathbf{P_e}\mathbf{G}_{\mathbf{\Omega c}}^{\mathbf{T}}]\mathbf{M}^{\star} \end{bmatrix} = \begin{bmatrix} \mathbf{j}_\mathbf{e}^{\circ} \\ \mathbf{j}_\mathbf{e}^{\star} \end{bmatrix} = \begin{bmatrix} \mathbf{M}^{\circ\mathbf{T}}\boldsymbol{e}_{ext} \\ \mathbf{M}^{\star\mathbf{T}}\boldsymbol{e}_{ext} \end{bmatrix}. \tag{84}$$

In the system above, the capacitive term is only present in the matrix block (2,2). Indeed, due to the properties $\mathbf{M}^{\star\mathbf{T}}\mathbf{M}^{\circ} = \mathbf{0}$ and $\mathbf{M}^{\circ\mathbf{T}}\mathbf{G}_{\mathbf{\Omega c}} = \mathbf{0}$, the capacitive term vanishes in all other matrix blocks. One can notice that in the (2,2) block of (84), there are still two terms which shows opposite behavior in frequency. However, the term $\mathbf{M}^{\star\mathbf{T}}\mathbf{L}\mathbf{M}^{\star}$ is much less significant compared to $\mathbf{M}^{\star\mathbf{T}}\frac{\mathbf{1}}{i\omega}\mathbf{G}_{\mathbf{\Omega c}}\mathbf{P_e}\mathbf{G}_{\mathbf{\Omega c}}^{\mathbf{T}}\mathbf{M}^{\star}$ and, when the frequency is low, it can be also completely removed (indeed, it models the *negligible* inductive effects due to the star unknowns).
Finally, by scaling the second row of (84) by $\omega^2\mu_0\varepsilon_0$, the breakdown in frequency issue can be removed and (with a further scaling of the polarization currents) the problem can be solved down to $\omega = 0$.
Obviously, a completely equivalent procedure can be applied when magnetic media are considered in the Coulombian PEEC formulation. Thus, thanks to this change of basis technique, a system of almost the same dimension of (27) (much smaller than (25) where the scalar potentials are kept as unknowns) can be adopted also for the study of low frequency EM problems avoiding the breakdown in frequency issue.
Finally, it is worth noting that when for some physical reason the divergence free condition $\boldsymbol{\nabla} \cdot \mathbf{J_e} = \mathbf{0}$ and $\mathbf{J_e} \cdot \mathbf{n} = \mathbf{0}$ must be strongly enforced (i.e. no volume or surface charge is present), the star matrix $\mathbf{M}^{\star}$ and the star unknowns $\mathbf{j}_\mathbf{e}^{\star}$ are not needed anymore. Instead, when $\boldsymbol{\nabla} \cdot \mathbf{J_e} = \mathbf{0}$ only must to be enforced (i.e. no volume charge) $\mathbf{M}^{\star}$ can be properly reduced and the $\mathbf{j}_\mathbf{e}^{\star}$ related to the volumes of the mesh can be neglected.
In conclusion of this paragraph, when the Amperian PEEC approach is adopted the above discussion can be obviously applied to $\mathbf{j_e}$. For the magnetization, instead, different considerations can be made. From Maxwell's equations, when homogeneous magnetic media are considered, following equation holds:

$$\boldsymbol{\nabla} \times \mathbf{M} = (\mu_r - 1)(\mathbf{J_c} + i\varepsilon_0\varepsilon_r\mathbf{D}). \tag{85}$$

From the above equation, it is clear that when the frequency is relatively low and the magnetic media is non-conductive, the curl of the magnetization is almost zero and thus $\mathbf{J_a} \approx \mathbf{0}$.
This means that $\mathbf{M}$ can be written as $\mathbf{M} = \nabla\psi$, where ψ is a scalar potential in Ω_m. Thus, from a discrete point of view, the column vector $\mathbf{m}$ can be written as:

$$\mathbf{m} = \mathbf{G}_{\mathbf{\Omega m}}\boldsymbol{\psi}, \tag{86}$$

where $\boldsymbol{\psi}$ is the column vector of the DoFs corresponding to ψ on the nodes of mesh (except one for each sub-region, considered as reference). Therefore, (86) can be applied to the third row of system (55) and $\mathbf{G}_{\mathbf{\Omega m}}^{\mathbf{T}}$ can be applied to project the new matrix equation onto a new set of linear equations. Thus, when non-conductive homogeneous magnetic media are considered, the property $\mathbf{J_a} = \boldsymbol{\nabla} \times \mathbf{M} \approx \mathbf{0}$ can be strongly imposed by using (86), which also reduces the number of unknowns and improves the sparsity of the magnetic equation in (55).

C. Solution Strategies

The PEEC system of equations can be solved by using different strategies, the efficiency of which depends on the characteristic of problem to be solved.
In the 70s, when the PEEC method was first proposed, due to the limited computing power, the studied systems were mostly small interconnects or PCB traces discretized with very coarse

meshes. Indeed, at that time the main interest on the PEEC method was the possibility to couple the (full Maxwell) EM problem with circuit problems (even very large ones) consisting of lumped components with limited connectivity between ports. When this kind of problems is considered, since the final (coupled) EM-circuit problem mainly consists of lumped components, it is natural to consider the problem in the context of electric circuits, rather than the one of EM fields. Thus, the most natural way to solve the final linear system is to adopt a Spice-like solver.

Typically, the input required by this kind of solvers is the *net list* of the electric circuit to be solved and then the problem is written in Modified Nodal Analysis (MNA) form and the final system of equations is actually assembled by the software itself. In most of cases, the connections between the components are limited, thus the resulting system of equations is very sparse (possibly very large). Indeed, the solvers adopted in Spice-like software are usually sparse direct ones, e.g. T. Davis's KLU. Therefore, when this solution strategy is chosen, the final PEEC system of equations to be solved is (40) (or (55) and (75) complemented by the lumped components for the case of the Amperian and Coulombian methods, respectively). Actually, the *net list* of the equivalent circuit (obtained from the discretization of the PEEC method coupled with the lumped elements) must be constructed and the resulting file is the input of the Spice-like software.

One of the main advantages of the use of a Spice-like solver is that many passive and active circuit component models are already implemented in the Spice software. Thus, the user can use them as *black box components* during the construction of the *net list*, which is a very attractive feature for some kind of applications.

As already stated, it is worth noting that (55), derived from the Amperian method, is not directly suitable to be written in MNA form. Indeed, the magnetic domains cannot be represented by means of the traditional PEEC elementary circuit branch and thus they must be further handled. Instead, the Coulombian formulation presented in section III.C proposed in [24] and [25] offers the same circuit interpretation of both electric and magnetic domains by means of the traditional PEEC elementary circuit cell (Fig. 4).

In [31] and [47], different ways to construct the *net list* from the equivalent PEEC circuit are shown. However, as clearly stated in these works, with the nowadays available computing power the application of an MNA Spice-like solver to the final EM-circuit system of equations is actually feasible only when the discretized objects are represented by a small number of equivalent electric branches (a few hundred). Indeed, the equivalent circuit components obtained from the PEEC discretization are fully mutually coupled. Thus, with the increase of the number of mesh elements the sparsity ratio of the systems decreases and the efficiency of sparse direct solvers drastically drops. Moreover, most of the Spice-like solvers allow a limited number of mutual connections between the lumped components. Furthermore, when many mutual connections are considered, the *net list* itself requires a considerable amount of disk space and reading time, which may dominate the total simulation time.

Finally, it is worth noting that both frequency and time domains simulations can be performed with Spice-like solvers by using the same equivalent circuit (i.e. the same *net list*). The Θ-method or other traditional numerical schemes can be adopted for the time domain simulations. However, when the dynamic Green's function is adopted (7) (i.e. retardation effects are considered) time domain analysis cannot be performed with traditional Spice-like software. Indeed, the Marching On-in-Time (MOT) scheme can be applied to the PEEC method in order to perform transient simulations considering the time delay effects in the propagation of the EM fields. A MOT-PEEC method based on the standard discretization scheme has been presented in [48] for conductive and dielectric media, while an unstructured MOT-PEEC method for conductive, dielectric, and magnetic media has been presented at the latest Compumag and is now submitted to the IEEE Transactions on Magnetics.

With the massive increase of computing power and available RAM for standard workstations, the interest in performing increasingly complex and computationally expensive EM simulations has risen steadily. For applications where the air meshing is computationally expensive or incurs in robustness issues, integral equation methods may be preferable to the Finite Element Method (FEM). The PEEC method offers all the advantages of the integral equation methods together with a useful circuit interpretation of the EM problem. Thus, when complex EM devices are coupled with lumped circuit components, the PEEC method becomes an attractive approach for their study. Because of the arguments stated above, when the meshing of the EM devices requires a relative high number of equivalent circuit branches, it is convenient to consider the problem in the context of EM fields, rather than electric circuits. Thus, since MNA Spice-like solvers cannot be efficiently used for the solution of coupled EM-circuit PEEC problems, different solution strategies must be adopted.

When the storage of the system matrix is not prohibitive in terms of memory consumption, (55) and (75) can be solved by means of a direct LU decomposition of the matrix. It is worth noting that, since the system of equations is symmetric (or can be symmetrized), only the lower triangular L matrix of the LU decomposition must be evaluated. The *ZGESV* routine of LAPACK (also present in the optimized Intel Math Kernel Library) can be adopted for an efficient solution of the final system of equations by means of the LU decomposition. However, since the computational cost of the LU decomposition requires $\sim N^3$ floating-point operations (where N is the system dimension), it is convenient to operate on a system of equations of the smallest possible size. Therefore, when the LU solution strategy is embraced, the more compact systems (27) and (84) are more attractive.

In recent years, the interest in using less demanding iterative solvers for the solution of the final PEEC system of equations has increased [12]. Indeed, the final purpose is to provide a method which allows for an (accurate) approximation of the solution with a computational cost reasonably smaller than the one required by the LU decomposition. However, good results can be obtained only when an appropriate preconditioner is adopted, which is currently a very sensitive issue. Interesting results and discussions have been presented in [12] where different preconditioning approaches have been investigated for different PEEC formulations. In the literature concerning Volume Integral Equation methods, the sparse resistive matrices are usually adopted as preconditioners [49], [50]. However, all these solutions are far from being general solutions and more sophisticated preconditioning approaches should be adopted [51]. For instance, incomplete-LU (ILU) preconditioning has been investigated in the literature in the context of scattering problems [52], [53].

The topic of robust and efficient preconditioning is still largely open and a completely general solution is probably not possible since the numerical nature of the final PEEC system of the equations is highly problem dependent.

Beyond the problem of the computational cost required for the solution of the final system of equations, the storage of the full matrix itself is a sensitive issue which must be considered. For all these reasons, from the perspective of the authors, the preconditioning topic should be investigated in the framework

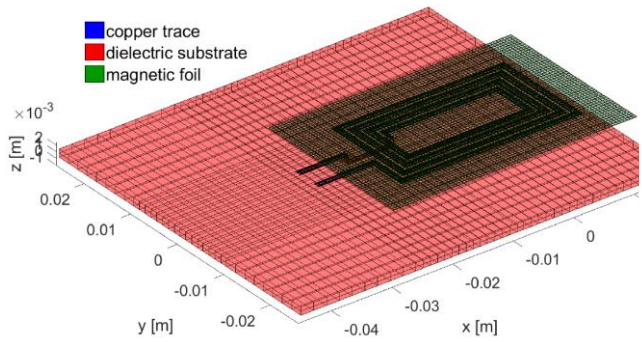

Fig. 6. NFC Antenna, PEEC model and mesh.

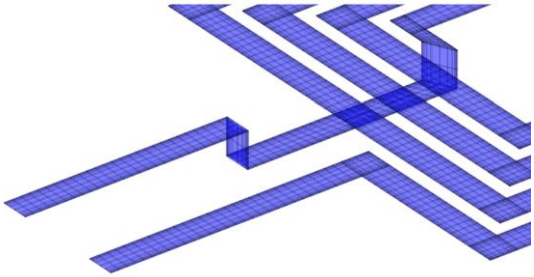

Fig. 7. NFC Antenna, detail of the PEEC model and mesh for the conductive copper trace.

of *low-rank approximation techniques* which allow the reduction of the memory requirement [3], [54].

The application of low-rank approximation techniques coupled with iterative solvers to solve PEEC systems of equations has been examined in different works. Indeed, for problems of practical interest, low-rank approximation approaches are often mandatory. Thus, iterative solvers combined with appropriate preconditioning techniques are actually useful only when combined with low-rank approximation methods, which allow to compress the matrix down to some percent with respect to the full one [55].

VI. Numerical Results

A 3-D code based on both the Amperian and Coulombian PEEC formulations has been developed with MATLAB® for the system assembly and data handling, while MEX-FORTRAN functions combined with OpenMP libraries have been adopted for the computation of the matrix coefficients and post-processing. Both tetrahedral and hexahedral elements are supported. Furthermore, both external EM fields and lumped elements can be considered as sources.

All simulations were run on a Linux machine equipped with dual 6-core/12-thread processors (Xeon E5-2643 v4 @3.40GHz) and 512 GB RAM.

The case of a real NFC antenna operating at f = 13.56 MHz, shown in Fig. 6 and Fig. 7 is considered [26], and results reported in this section are also presented in [24]. The device consists of a copper trace ($\sigma_c = 57 \cdot 10^6$ S/m, 35 μm thick, 1 mm wide) placed on a FR4 dielectric substrate ($\varepsilon_r = 4.3$). The coil has outer dimensions of 30 mm × 17 mm, while the FR4 substrate is 61 mm × 52 mm wide, with a thickness of 1.35 mm. A ferrite foil (μ_r = 163, 40 mm × 27 mm wide and with a thickness of 100 μm) is placed on top of the copper trace in order to reduce the detuning effects due to eddy currents.

The device is discretized with hexahedral elements and a lumped voltage source is connected to the quadrilateral faces that discretize the terminals of the conductive antenna by means of short circuit branches.

TABLE I. EQUIVALENT IMPEDANCE OF THE NFC ANTENNA.

	Z_{eq} *mod.1* [Ω]	Z_{eq} *mod.2* [Ω]
Measured	$0.46 + i55.39$	$0.36 + i34.82$
Coulombian PEEC	$0.45 + i55.18$	$0.37 + i34.39$
FEM	$0.44 + i55.06$	$0.36 + i34.46$
IE	$0.33 + i57.65$	$0.33 + i35.52$
Amperian PEEC	$0.39 + i35.93$	$0.37 + i34.39$

Table I shows the values of the equivalent impedance Z_{eq} obtained from the Amperian and Coulombian methods which are compared with measurements [26], with the values obtained from COMSOL® (a well-known FEM software), and a well-known commercial software (IE) based on IEM. For this study the device was modelled both with (*mod.1*) and without (*mod.2*) the presence of the ferrite foil.

It can be noticed that the results obtained from Coulombian PEEC are in good agreement with measured values and that the proposed PEEC method well identifies the influence of the thin magnetic foil on the value of the active losses (i.e. real part of Z_{eq}). Conversely, Amperian PEEC seems not to provide an accurate value of Z_{eq}. This behavior often emerges when thin magnetic objects are placed very close to conductive media. As noted also from other simulations, this is probably due to a too coarse discretization of the magnetic foil along the thickness direction and to the numerical issue discussed above for media with high permeability values. However, in order to allow a fair comparison between the proposed and the traditional PEEC methods, the same mesh and the same precision for the evaluation of the matrix coefficients were adopted for both Coulombian and Amperian methods.

Fig. 8 shows the magnitude of Z_{eq} in the frequency range computed by the Coulombian PEEC code and the commercial software.

Furthermore, the electric and magnetic fields produced by the device along an ellipse surrounding the NFC antenna are evaluated and compared with the results obtained from the FEM code and results in terms of the (complex) magnitudes of the magnetic and electric fields are shown in Fig. 9.

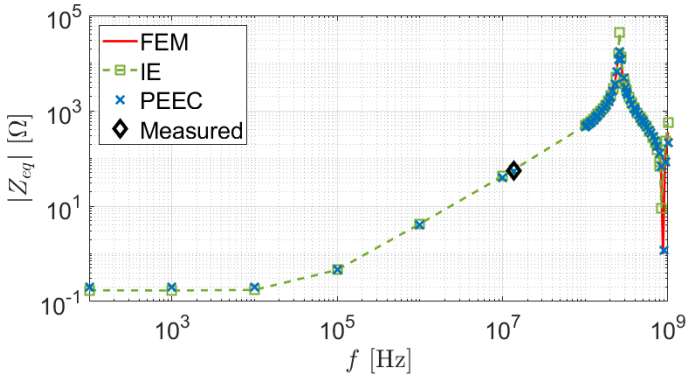

Fig. 8. $|Z_{eq}|$ of *mod.1* in the frequency range.

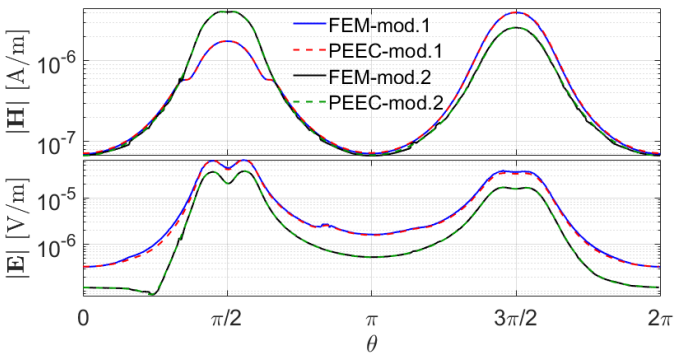

Fig. 9. Complex norm of **H** and **E** along the elliptical line

Table I, Fig. 8, and Fig. 9 show a good agreement between the results obtained from the implemented Coulombian PEEC code, measurements, and the commercial software.

Concerning the computational cost, the model adopted for the FEM simulations consists of a large number of elements since very thin volumetric objects, such as the copper trace and the magnetic foil, are discretized. Fig. 10 and Fig. 11 show a detail of the mesh adopted for the FEM model, which consists of $\sim 6.2 \cdot 10^6$ tetrahedral elements and 5,508 prisms (for the Perfectly Match Layer condition), leading to $\sim 39.3 \cdot 10^6$ DoFs. The solution of the problem, with a FGMRES solver with a relative tolerance of 10^{-7}, required 4,230 s of simulation time with a peak memory usage (PMU) of 235 GB.

On the hand, the Coulombian PEEC method required a relatively small number of hexahedral elements for the discretization of the conductive, dielectric, and magnetic domains. In particular, a very coarse mesh consisting of 322 conducting, 1,374 dielectric, and 2,852 magnetic hexahedral elements was sufficient to attain a very good accuracy in terms of the produced EM fields. Indeed, concerning the evaluation of the EM fields, one element carrying a (mean) value of the conduction current density was sufficient for the discretization of the cross section of the copper trace. The total number of DoFs of the assembled system was 17,335. Since only homogeneous media were considered, the change of basis procedure discussed in section IV.C (without volume star currents) was adopted, leading to 12,789 DoFs for the system to be solved in the reduced basis. The simulation time was 98 s with a PMU of 10.7 GB. On the other hand, the accurate evaluation of the real part of the equivalent impedance (related to the power losses) required a larger amount of elements for the discretization of the copper trace, since it was necessary to obtain a good approximation of the correct distribution of the conduction current density vector, which is strongly affected by proximity effects. Thus, the model adopted for the Coulombian PEEC code for the evaluation of Z_{eq} consisted of 6,480 conducting, 1,374 dielectric, and 12,060 magnetic hexahedral elements, leading to a total number of 81,059 DoFs for the assembled system, 59,669 for the system to be solved, a simulation time of 4,817 s, and a PMU of 56 GB. The PEEC system was solved with an LU decomposition.

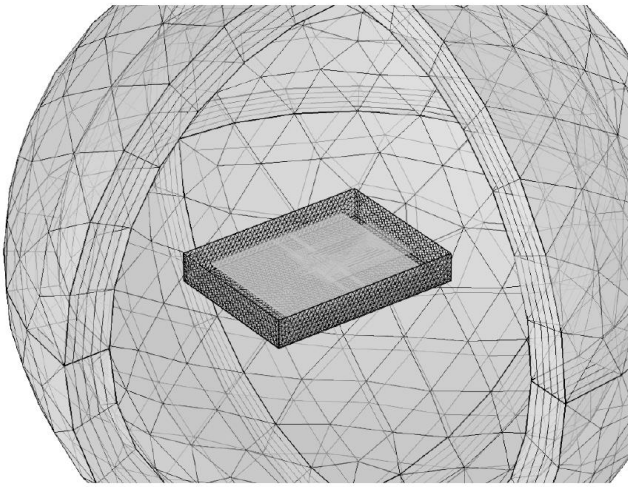

Fig. 10. FEM mesh of the NFC antenna.

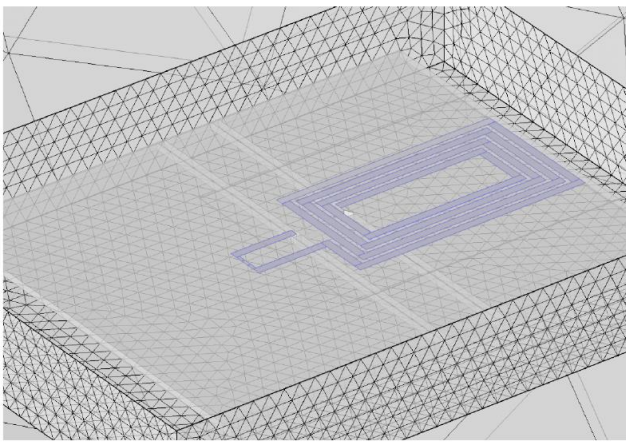

Fig. 11. FEM mesh of the NFC antenna, detail.

In the case of the commercial IE software, since lumped voltage sources can only be applied to interior edges of surface models, an equivalent surface model has been adopted for the copper trace and the two terminals of the antenna have been *physically* connected. The computational cost has been comparable with the PEEC one (coarse case). However, probably because of the use of an equivalent surface model, the real part of Z_{eq} seems not to be influenced by the presence of the magnetic foil, even when finer meshes are adopted, which is an issue if the focus of the simulation is on the losses.

Instead, with the 3-D Coulombian PEEC code, volume models can be naturally connected to lumped circuit elements allowing the proper evaluation of the losses of the NFC antenna, which is an important quantity to be considered during the design process.

Finally, to demonstrate the applicability and efficiency of compression techniques for the solution of the PEEC problem, the HLIBPro library, based on H^2 matrix representation and ACA, has been coupled with the Coulombian PEEC code to solve the NFC antenna problem, as proposed in [3].

The compression tolerance and the admissibility value (see [3] for their definition) are $\epsilon_{ACA} = 10^{-7}$ and $\eta = 2$, respectively. This, with respect the computation cost of the PEEC method (finer case) given above, lead to a $\sim 6.8\%$ compression ratio for the storage of the compressed system (i.e. down to 3.8 GB from 56 GB) and a computation time of ~ 73 s for the construction of the compressed system. The construction of the H-LU, obtained by imposing the same tolerance $\epsilon_{ACA} = 10^{-7}$, required almost the same memory and time required for the construction of the compressed system. Finally, the GMRES solver preconditioned with the H-LU only required 7 iterations and ~12 s of computation time (for a total simulation time of 155 s vs. 4818 s without low rank approximation). The error obtained in the final solution, with respect the one obtained from the uncompressed system, was $\sim 0.73\%$.

VI. Conclusions and Outlooks

The Partial Element Equivalent Circuit (PEEC) method, deeply rooted in (Volume) Integral Equation Methods, is by no means novel, however, fairly recent extensions to more general materials and extended frequency range, and advances in Low Rank Approximation approaches are spurring increasing interest. Due to these advancements in generality and efficiency, PEEC is starting to become more of a general-purpose tool and less of a niche technique. In the context of our research group, we plan to apply PEEC to the study of several electromagnetic devices of automotive interest, including Wireless Power Transfer ones, and to the study of complex devices of interest in the Nuclear Fusion community.

It is our belief that PEEC will further become a mainstream numerical technique for the solution of challenging engineering problems and that it will remain relevant for the Compumag community in the years to come.

Sample codes are available at
https://github.com/UniPD-DII-ETCOMP/DenseMatrixMarket

VII. Acknowledgements

Some parts of this article have been derived from [24], © 2019 IEEE. Reprinted, with permission, from [24]. The authors wish to thank the IEEE for the license.

VI. References

[1] M. Bebendorf, *Hierarchical Matrices: A Means to Efficiently Solve Elliptic Boundary Value Problems*. Berlin Heidelberg: Springer-Verlag, 2008.

[2] K. Zhao, M. N. Vouvakis, and J.-F. Lee, "The adaptive cross approximation algorithm for accelerated method of moments computations of EMC problems," *IEEE Transactions on Electromagnetic Compatibility*, vol. 47, no. 4, pp. 763–773, Nov. 2005.

[3] D. Voltolina, P. Bettini, P. Alotto, F. Moro, and R. Torchio, "High-Performance PEEC Analysis of Electromagnetic Scatterers," *IEEE Transactions on Magnetics*, vol. 55, no. 6, pp. 1–4, Jun. 2019.

[4] A. E. Ruehli, "Inductance Calculations in a Complex Integrated Circuit Environment," *IBM Journal of Research and Development*, vol. 16, no. 5, pp. 470–481, Sep. 1972.

[5] D. Romano and G. Antonini, "Partial Element Equivalent Circuit-Based Transient Analysis of Graphene-Based Interconnects," *IEEE Transactions on Electromagnetic Compatibility*, vol. 58, no. 3, pp. 801–810, Jun. 2016.

[6] D. Romano, I. Kovacevic-Badstubner, M. Parise, U. Grossner, J. Ekman, and G. Antonini, "Rigorous DC Solution of Partial Element Equivalent Circuit Models Including Conductive, Dielectric, and Magnetic Materials," *IEEE Transactions on Electromagnetic Compatibility*, pp. 1–10, 2019.

[7] T. Bauernfeind *et al.*, "Multi-Objective Synthesis of NFC-Transponder Systems Based on PEEC Method," *IEEE Transactions on Magnetics*, vol. 54, no. 3, pp. 1–4, Mar. 2018.

[8] P. Baumgartner *et al.*, "Multi-Objective Optimization of Yagi–Uda Antenna Applying Enhanced Firefly Algorithm With Adaptive Cost Function," *IEEE Transactions on Magnetics*, vol. 54, no. 3, pp. 1–4, Mar. 2018.

[9] A. E. Ruehli et al., *Circuit Oriented Electromagnetic Modeling Using the PEEC Techniques*. John Wiley & Sons, Inc., June 2017.

[10] R. Torchio, D. Voltolina, P. Alotto, P. Bettini, and F. Moro, "The Partial Element Equivalent Circuit Method for High Frequency Problems," in *Compendium on Electromagnetic Analysis, From Electrostatics to Photonics: Fundamentals and Applications for Physicists and Engineers*, World Scientific, 2020.

[11] J. Ekman, *Electromagnetic modeling using the partial element equivalent circuit method*, Ph.D. dissertation, Embedded Internet Systems Lab, Lulea University of Technology, 2016.

[12] J. Siau, *Unstructured PEEC formulations considering resistive, inductive and capacitive effects for power electronics*, Ph.D. dissertation, Université Grenoble Alpes, 2016.

[13] R. Torchio, *Extending the Unstructured PEEC Method to Magnetic, Transient, and Stochastic Electromagnetic Problems*. Ph.D. dissertation, Univeristà degli Studi di Padova and Université Grenoble Alpes, 2019.

[14] V. Ardon, J. Aime, O. Chadebec, E. Clavel, J. Guichon, and E. Vialardi, "EMC Modeling of an Industrial Variable Speed Drive With an Adapted PEEC Method," *IEEE Transactions on Magnetics*, vol. 46, no. 8, pp. 2892–2898, Aug. 2010.

[15] D. Romano and G. Antonini, "Augmented Quasi-Static Partial Element Equivalent Circuit Models for Transient Analysis of Lossy and Dispersive Magnetic Materials," *IEEE Transactions on Magnetics*, vol. 52, no. 5, pp. 1–11, May 2016.

[16] I. F. Kovačević, T. Friedli, A. M. Müsing, and J. W. Kolar, "Full PEEC Modeling of EMI Filter Inductors in the Frequency Domain," *IEEE Transactions on Magnetics*, vol. 49, no. 10, pp. 5248–5256, Oct. 2013.

[17] G. Antonini, A. E. Ruehli, and J. Esch, "Nonorthogonal PEEC formulation for time and frequency domain modeling," in *2002 IEEE International Symposium on Electromagnetic Compatibility*, 2002, vol. 1, pp. 452–456 vol.1.

[18] F. Freschi, and M. Repetto, "A General Framework for Mixed Structured/Unstructured PEEC Modelling," Applied Computational Electromagnetics Society Journal Vol. 23, No. 3., pp. 200–206, 2008.

[19] J. Siau, G. Meunier, O. Chadebec, J. Guichon, and R. Perrin-Bit, "Volume Integral Formulation Using Face Elements for Electromagnetic Problem Considering Conductors and Dielectrics," *IEEE Transactions on Electromagnetic Compatibility*, vol. 58, no. 5, pp. 1587–1594, Oct. 2016.

[20] R. Torchio, P. Alotto, P. Bettini, D. Voltolina, and F. Moro, "A 3-D PEEC Formulation Based on the Cell Method for Full-Wave Analyses With Conductive, Dielectric, and Magnetic Media," *IEEE Transactions on Magnetics*, vol. 54, no. 3, pp. 1–4, Mar. 2018.

[21] E. Verbeek, "Partial element equivalent circuit (PEEC) models for on-chip passives and interconnects," International Journal of Numerical Modelling: Electronic Networks, Devices and Fields, vol. 17, no. 1, 2004.

[22] G. Antonini, M. Sabatini, and G. Miscione, "PEEC modeling of linear magnetic materials," in *2006 IEEE International Symposium on Electromagnetic Compatibility, 2006. EMC 2006.*, 2006, vol. 1, pp. 93–98.

[23] D. Romano and G. Antonini, "Quasi-Static Partial Element Equivalent Circuit Models of Linear Magnetic Materials," *IEEE Transactions on Magnetics*, vol. 51, no. 7, pp. 1–15, Jul. 2015.

[24] R. Torchio, "A Volume PEEC Formulation Based on the Cell Method for Electromagnetic Problems from Low to High Frequency," *IEEE Transactions on Antennas and Propagation*, pp. 1–13, 2019.

[25] R. Torchio, F. Moro, G. Meunier, J.-M. Guichon, and O. Chadebec, "An Extension of Unstructured-PEEC Method to Magnetic Media," *IEEE Transactions on Magnetics*, vol. 55, no. 6, pp. 1–4, Jun. 2019.

[26] T. Bauernfeind, K. Preis, W. Renhart, O. Bíró, and M. Gebhart, "Finite Element Simulation of Impedance Measurement Effects of NFC Antennas," *IEEE Transactions on Magnetics*, vol. 51, no. 3, pp. 1–4, Mar. 2015.

[27] R. Kriemann, "HLIBPro (v.2.6). Accessed: Nov. 1, 2017. [Online]. Available: http://www.hlibpro.com.".

[28] Adams Stratton Julius., *Electromagnetic Theory*. Mcgraw Hill Book Company, 1941.

[29] J.-S. Zhao and W. C. Chew, "Integral equation solution of Maxwell's equations from zero frequency to microwave frequencies," *IEEE Transactions on*

Antennas and Propagation, vol. 48, no. 10, pp. 1635–1645, Oct. 2000.
[30] P. Yla-Oijala, J. Markkanen, S. Jarvenpaa, and S. P. Kiminki, "Surface and Volume Integral Equation Methods for Time-Harmonic Solutions of Maxwell's Equations (Invited Paper)," *Progress In Electromagnetics Research*, vol. 149, pp. 15–44, 2014.
[31] F. Freschi, "Fast Block-Solution of PEEC Equations," *IEEE Transactions on Magnetics*, vol. 49, no. 5, pp. 1753–1756, May 2013.
[32] F. P. Andriulli, "Loop-Star and Loop-Tree Decompositions: Analysis and Efficient Algorithms," *IEEE Transactions on Antennas and Propagation*, vol. 60, no. 5, pp. 2347–2356, May 2012.
[33] P. Alotto, F. Freschi, M. Repetto, and C. Rosso, *The Cell Method for Electrical Engineering and Multiphysics Problems: An Introduction*. Berlin Heidelberg: Springer-Verlag, 2013.
[34] L. Codecasa, "Refoundation of the Cell Method Using Augmented Dual Grids," *IEEE Transactions on Magnetics*, vol. 50, no. 2, pp. 497–500, Feb. 2014.
[35] A. Bossavit, *Computational Electromagnetism*. Academic Press, 1998.
[36] P. Dular, R. Specogna, and F. Trevisan, "Constitutive Matrices Using Hexahedra in a Discrete Approach for Eddy Currents," *IEEE Transactions on Magnetics*, vol. 44, no. 6, pp. 694–697, Jun. 2008.
[37] M. Fabbri, "Magnetic Flux Density and Vector Potential of Uniform Polyhedral Sources," *IEEE Transactions on Magnetics*, vol. 44, no. 1, pp. 32–36, Jan. 2008.
[38] S. Järvenpää, M. Taskinen, and P. Ylä-Oijala, "Singularity extraction technique for integral equation methods with higher order basis functions on plane triangles and tetrahedra," *International Journal for Numerical Methods in Engineering*, vol. 58, no. 8, pp. 1149–1165, 2003.
[39] H. Heeb and A. E. Ruehli, "Three-dimensional interconnect analysis using partial element equivalent circuits," *IEEE Transactions on Circuits and Systems I: Fundamental Theory and Applications*, vol. 39, no. 11, pp. 974–982, Nov. 1992.
[40] A. M. Turing, "Rounding-Off Errors in Matrix Process", Q. J. Mech. Appl. Math., vol. 1, no. 287, 1948.
[41] R. Torchio, P. Alotto, P. Bettini, D. Voltolina, and F. Moro, "A DC to HF volume PEEC formulation based on hertz potentials and the cell method," in *2018 International Applied Computational Electromagnetics Society Symposium (ACES)*, 2018, pp. 1–2.
[42] R. M. Fano et al., *Electromagnetic Fields, Energy, and Forces*. M.I.T. Press, 1960.
[43] A. Nisbet and E. T. Whittaker, "Hertzian electromagnetic potentials and associated gauge transformations," *Proceedings of the Royal Society of London. Series A. Mathematical and Physical Sciences*, vol. 231, no. 1185, pp. 250–263, Aug. 1955.
[44] A. E. Seaver, "Some Comments on the Charge Decay Paradox in Metals", *Proc. ESA Annual Meeting on Electrostatics*, Paper D4 2008.
[45] C. Forestiere, G. Miano, G. Rubinacci, A. Tamburrino, L. Udpa, and S. Ventre, "A Frequency Stable Volume Integral Equation Method for Anisotropic Scatterers," *IEEE Transactions on Antennas and Propagation*, vol. 65, no. 3, pp. 1224–1235, Mar. 2017.
[46] P. Dłotko and R. Specogna, "Physics inspired algorithms for (co)homology computations of three-dimensional combinatorial manifolds with boundary," *Computer Physics Communications*, vol. 184, no. 10, pp. 2257–2266, Oct. 2013.
[47] S. Sohrab, and E. Jonas, "Feasibility analysis of specialized PEEC solvers in comparison to SPICE-like solvers", *Journal of Computational Electronics*, vol. 11, no. 4, pp. 440–452, 2012.
[48] C. Gianfagna, L. Lombardi, and G. Antonini, "Marching-on-in-time solution of delayed PEEC models of conductive and dielectric objects," *Antennas Propagation IET Microwaves*, vol. 13, no. 1, pp. 42–47, 2019.
[49] J. Markkanen, P. Ylä-Oijala, and S. Järvenpää, "On the spectrum and preconditioning of electromagnetic volume integral equations," in *2016 URSI International Symposium on Electromagnetic Theory (EMTS)*, 2016, pp. 834–837.
[50] R. Misawa et al., "Preconditioning of Periodic Fast Multipole Method for Solving Volume Integral Equations," *IEEE Transactions on Antennas and Propagation*, vol. 62, no. 9, pp. 4799-4804, Sept. 2014.
[51] T. Xia *et al.*, "An Enhanced Augmented Electric-Field Integral Equation Formulation for Dielectric Objects," *IEEE Transactions on Antennas and Propagation*, vol. 64, no. 6, pp. 2339–2347, Jun. 2016.
[52] J. Lee, J. Zhang, and C.-C. Lu, "Incomplete LU preconditioning for large scale dense complex linear systems from electromagnetic wave scattering problems," *Journal of Computational Physics*, vol. 185, no. 1, pp. 158–175, Feb. 2003.
[53] P. Yla-Oijala and M. Taskinen, "Well-conditioned Muller formulation for electromagnetic scattering by dielectric objects," *IEEE Transactions on Antennas and Propagation*, vol. 53, no. 10, pp. 3316–3323, Oct. 2005.
[54] R. Torchio, P. Bettini, and P. Alotto, "PEEC-Based Analysis of Complex Fusion Magnets During Fast Voltage Transients With H-Matrix Compression," *IEEE Transactions on Magnetics*, vol. 53, no. 6, pp. 1–4, Jun. 2017.
[55] P. Alotto, P. Bettini, and R. Specogna, "Sparsification of BEM Matrices for Large-Scale Eddy Current Problems," *IEEE Transactions on Magnetics*, vol. 52, no. 3, pp. 1–4, Mar. 2016.

AUTHORS NAME AND AFFILIATION

All authors are with the Department of Industrial Engineering of the University of Padova, Italy.

Piergiorgio Alotto, piergiorgio.alotto@unipd.it
Paolo Bettini, paolo.bettini@unipd.it
Federico Moro, federico.moro@unipd.it
Riccardo Torchio, riccardo.torchio@studenti.unipd.it
Dimitri Voltolina, dimitri.voltolina@studenti.unipd.it